

1 On the formation of highly oxidized pollutants by autoxidation of 2 terpenes under low temperature combustion conditions: the case 3 of limonene and α -pinene.

4 Roland Benoit¹, Nesrine Belhadj^{1,2}, Zahraa Dbouk^{1,2}, Maxence Lailliau^{1,2}, and Philippe Dagaut¹

5 ¹CNRS-INSIS, ICARE, Orléans, France, roland.benoit@cnrs-orleans.fr, nesrine.belhadj@cnrs-orleans.fr,
6 zahraa.dbouk@cnrs-orleans.fr, maxence.lailliau@cnrs-orleans.fr, dagaut@cnrs-orleans.fr

7 ²Université d'Orléans, Orléans, France

8 **Correspondance:** Roland Benoit (roland.benoit@cnrs-orleans.fr)

9

10 **Abstract.**

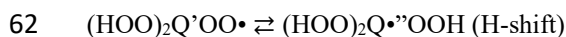
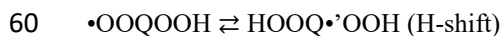
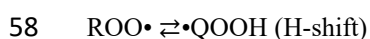
11 The oxidation of monoterpenes under atmospheric conditions has been the subject of numerous studies. They were
12 motivated by the formation of oxidized organic molecules (OOM) which, due to their low vapor pressure, contribute
13 to the formation of secondary organic aerosols (SOA). Among the different reaction mechanisms proposed for the
14 formation of these oxidized chemical compounds, it appears that the autoxidation mechanism, involving successive
15 events of O₂ addition and H-migration, common to both low-temperature combustion and atmospheric conditions, is
16 leading to the formation of highly oxidized products (HOPs). However, cool flame oxidation (~500-800 K) of terpenes
17 has not received much attention even if it can contribute to atmospheric pollution through biomass burning and
18 wildfires. Under such conditions, terpenes can be oxidized via autoxidation. In the present work, we performed
19 oxidation experiments with limonene-oxygen-nitrogen and α -pinene-oxygen-nitrogen mixtures in a jet-stirred reactor
20 (JSR) at 590 K, a residence time of 2 s, and atmospheric pressure. Oxidation products were analyzed by liquid
21 chromatography, flow injection, and soft ionization-high resolution mass spectrometry. H/D exchange and 2,4-
22 dinitrophenyl hydrazine derivatization were used to assess the presence of OOH and C=O groups in oxidation products,
23 respectively. We probed the effects of the type of ionization used in mass spectrometry analyses on the detection of
24 oxidation products. Heated electrospray ionization (HESI) and atmospheric pressure chemical ionization (APCI), in
25 positive and negative modes were used. We built an experimental database consisting of literature data for atmospheric
26 oxidation and presently obtained combustion data for the oxidation of the two selected terpenes. This work showed a
27 surprisingly similar set of oxidation products chemical formulas, including oligomers, formed under the two rather
28 different conditions, i.e., cool flame and simulated atmospheric oxidation. Data analysis (in HESI mode) indicated that
29 a subset of chemical formulas is common to all experiments, independently of experimental conditions. Finally, this
30 study indicates that more than 45% of the detected chemical formulas in this full dataset can be ascribed to an
31 autoxidation reaction.

32

33 1 Introduction

34 Terpenes are emitted into the troposphere by vegetation (Seinfeld and Pandis, 2006). They can be used as drop in fuels
 35 (Harvey et al., 2010;Mewalal et al., 2017;Harvey et al., 2015) which could increase emissions via fuel evaporation
 36 and unburnt fuel release. Biomass burning and wildfires can also release terpenes and their products of oxidation into
 37 the troposphere (Gilman et al., 2015;Hatch et al., 2019;Schneider et al., 2022). Wildfires temperature ranges from 573
 38 to 1373 K (Wotton et al., 2012), which covers both the cool flame (~500-800 K) and intermediate to high temperature
 39 combustion regimes. Products of biomass burning have been characterized earlier (Smith et al., 2009). Using van
 40 Krevelen diagrams, the authors reported H/C versus O/C in the ranges 0.5 to 3 and 0 to 1, respectively. Whereas a
 41 large fraction of these products can derive from cellulose, hemicellulose, and lignin oxidation, their formation via
 42 terpenes oxidation cannot be ruled out. In a more recent study (Gilman et al., 2015), it was reported that biomass
 43 burning emissions were dominated by oxidized organic compounds (57 to 68% of total mass emissions). Wildfires
 44 are getting more and more frequent and their intensity increases(Burke et al., 2021). In large wildfires, there are many
 45 updrafts which can transport a variety of materials ranging from gases to particulates, and even bacteria (Kobziar et
 46 al., 2018). Furthermore, it was recently demonstrated that recent wildfires in Australia produced smoke which could
 47 reach an altitude of 35 km (Khaykin et al., 2020). Such events could contribute to ozone destruction (Bernath et al.,
 48 2022) but also to tropospheric pollution. But, field measurements are not appropriate for comparison with the present
 49 data because a strict distinction on the origins of the chemical compounds observed cannot be assessed. For example,
 50 literature works and reviews (Hu et al., 2018;Popovicheva et al., 2019;Prichard et al., 2020) present field measurements
 51 from smoldering fires which were not detailed enough to be used here.

52 Cool flame oxidation is dominated by autoxidation (Bailey and Norrish, 1952;Benson, 1981;Cox and Cole,
 53 1985;Korcek et al., 1972) which involves peroxy radicals (ROO[•]). Autoxidation is based on an H-shift and oxygen
 54 addition which starts with the initial production of ROO[•] radicals. This mechanism can repeat itself several times and
 55 lead to recurrent oxygen additions to form highly oxidized products (Wang et al., 2017;Wang et al., 2018;Belhadj et
 56 al., 2020;Belhadj et al., 2021a;Belhadj et al., 2021b):



64 There, the formation of highly oxidized products (HOPs) was mainly attributed to autoxidation reactions (Belhadj et
 65 al., 2021c;Benoit et al., 2021).

66 In atmospheric chemistry, it is only relatively recently that this pathway has been considered (Vereecken et al.,
 67 2007;Crounse et al., 2013;Jokinen et al., 2014a;Ehn et al., 2014;Berndt et al., 2015;Jokinen et al., 2015;Berndt et al.,
 68 2016;Iyer et al., 2021). Also, it has been identified that highly oxygenated organic molecules (HOMs), a source of
 69 secondary organic aerosols (SOA), can result from autoxidation processes (Ehn et al., 2014;Wang et al., 2021;Tomaz
 70 et al., 2021;Bianchi et al., 2019). Modeling studies complemented by laboratory experiments showed that autoxidation

71 mechanisms proceed simultaneously on different ROO[•] radicals leading to the production of a wide range of oxidized
72 compounds in a few hundredths of a second (Jokinen et al., 2014a; Berndt et al., 2016; Bianchi et al., 2019; Iyer et al.,
73 2021). Recent works have shown that, under certain atmospheric conditions, this autoxidation mechanism could be
74 competitive with other reaction pathways involving ROO[•] radicals (Bianchi et al., 2019), e.g., the carbonyl channel
75 (ROO[•] → R_HO + OH), the hydroperoxide channel (ROO[•] + HOO[•] → ROOH + O₂ and RO[•] + [•]OH + O₂),
76 disproportionation reactions (ROO[•] + R'OO[•] → RO[•] + R'O[•] + O₂ and R_HO + R'OH + O₂), accretion reactions (ROO[•]
77 + R'OO[•] → ROOR' + O₂). Similarity, in terms of observed chemical formulas of products from cool flame oxidation
78 of limonene and atmospheric oxidation of limonene, has been reported recently (Benoit et al., 2021). The same year,
79 Wang et al. showed that the oxidation of alkanes follows this autoxidation mechanism under both atmospheric and
80 combustion conditions (Wang et al., 2021). Also, that work confirmed that internal H-shifts in autoxidation can be
81 promoted by the presence of functional groups, as predicted earlier (Otkjær et al., 2018) for ROO[•] radicals containing
82 OOH, OH, OCH₃, CH₃, C=O, or C=C groups. Autoxidation will preferentially form chemical functions such as
83 carbonyls, hydroperoxyl, or peroxy. This large diversity of chemical functions will promote the formation of isomers.
84 Nevertheless, the common point to these chemical compounds is the sequential addition of O₂. Therefore, in a database,
85 potential candidate products of autoxidation are easily identified by this sequential addition.

86 To better understand the importance of these reaction pathways, the experimental conditions unique to these two
87 chemistries must be considered. In laboratory studies conducted under simulated atmospheric conditions, oxidation
88 occurs at near-ambient temperatures (250-300 K), at atmospheric pressure, in the presence of ozone and/or [•]OH
89 radicals (Table S1), used to initiate oxidation with low initial terpene concentrations. In combustion, the [•]OH radical,
90 temperature, and pressure are driving autoxidation. In addition to the increase in temperature, the initial concentrations
91 of the reagents are generally higher compared to the atmospheric conditions, in order to initiate the oxidation with O₂,
92 which is much slower than that involving ozone or [•]OH. Rising temperature increases isomerization rates and favors
93 autoxidation, at the expense of other possible reactions of ROO[•] radicals. Indeed, it has been reported earlier that a
94 temperature rise from 250 to 273K does not affect the distribution of HOMs (Quéléver et al., 2019) whereas Tröstl et al.
95 suggested that the distribution of HOMs is affected by temperature, α-pinene or particle concentration (Tröstl et al.,
96 2016). Similarly, the experiments of Huang et al. performed at different temperatures (223 K and 296 K) and precursor
97 concentration (α-pinene 0.714 and 2.2 ppm) suggested that the physicochemical properties, such as the composition
98 of the oligomers (at the nanometer scale), can be affected by a variation of temperature (Huang et al., 2018). The broad
99 range of chemical molecules formed and the impact of the experimental conditions on their character remains a subject
100 for atmospheric chemistry as well as for combustion chemistry studies. Whatever the mechanism of aerosols
101 formation, i.e., oligomerization, functionalization, or accretion, their composition will be linked to that of the initial
102 radical pool (Camredon et al., 2010; Meusinger et al., 2017; Tomaz et al., 2021).

103 In low-temperature combustion, when the temperature is increased, fuel's autoxidation rate goes through a maximum
104 between 500 and 670 K, depending on the nature of the fuel (Belhadj et al., 2020; Belhadj et al., 2021c). In low-
105 temperature combustion chemistry as in atmospheric chemistry, the oxidation of a chemical compound leads to the
106 formation of several thousands of chemical products which result from successive additions of oxygen, isomerization,
107 accretion, fragmentation, and oligomerization (Benoit et al., 2021; Belhadj et al., 2021b). The exhaustive analysis of
108 chemical species remains, under the current instrumental limitations, impossible. Indeed, this would consist in
109 analyzing several thousands of molecules using separative techniques such as ultra-high-pressure liquid
110 chromatography (UHPLC) or ion mobility spectrometry (IMS) (Krechmer et al., 2016; Kristensen et al., 2016).

111 Nevertheless, it is possible to classify these molecular species, considering only $C_xH_yO_z$ compounds, according to
112 criteria accessible via graphic tools representation such as van Krevelen diagrams, double bond equivalent number
113 (DBE), and average carbon oxidation state (OSc) versus the number of carbon atoms (Kourtchev et al., 2015;Nozière
114 et al., 2015). Such postprocessing of large datasets has the advantage of immediately highlighting classes of
115 compounds or physicochemical properties such as the condensation of molecules (vapor pressure), the large variety
116 of oxidized products ($C_xH_yO_{1 \text{ to } 15}$ in the present experiments) and the formation of oligomers (Kroll et al., 2011;Xie et
117 al., 2020).

118 In addition to the recent studies focusing on the first steps of autoxidation, a more global approach, based on the
119 comparison of possible chemical transformations related to autoxidation in low temperature combustion and
120 atmospheric chemistry, is needed for evaluating the importance of autoxidation under tropospheric and low-
121 temperature combustion conditions. In order to study the effects of experimental conditions on the diversity of
122 chemical molecules formed by autoxidation, we have selected α -pinene and limonene, two isomeric terpenes among
123 the most abundant in the troposphere (Zhang et al., 2018). Limonene has a single ring structure and two double bonds,
124 one of which is exocyclic. α -Pinene has a bicyclic structure and a single endo-cyclic double bond. These two isomers
125 with their distinctive physicochemical characters are good candidates for studying autoxidation versus initial chemical
126 structure and temperature. For α -pinene, in addition to the reactivity of its endo-cyclic double bond, products of ring
127 opening of the cyclobutyl group have been detected (Kurtén et al., 2015;Iyer et al., 2021), which could explain the
128 diversity of observed oxidation products. This large pool of oxidation products is increased in the case of limonene by
129 the presence of two double bonds (Hammes et al., 2019;Jokinen et al., 2015).

130 The present work extends that concerning the oxidation of limonene alone (Benoit et al., 2021). Compared to previous
131 works, we have added the study of α -pinene oxidation to that of limonene and investigated the impact of ionization
132 modes on the number of molecules detected and their chemical nature (unsaturation, oxidation rate). The size of the
133 experimental and bibliographic databases has been increased by more than 50%, in particular by adding data specific
134 to autoxidation (Krechmer et al., 2016;Tomaz et al., 2021) and references on α -pinene (Tab. 2)). Here, we oxidized
135 α -pinene and limonene in a jet-stirred reactor at atmospheric pressure, excess of oxygen, and elevated temperature.
136 We characterized the impact of using different ionization techniques (HESI and APCI) in positive and negative modes
137 on the pool of detected chemical formulas. The particularities of each ionization mode were analyzed to identify the
138 most suitable ionization technique for exploring the formation of autoxidation products under low temperature
139 combustion. H/D exchange and 2,4-dinitrophenyl hydrazine derivatization were used to assess the presence of
140 hydroperoxy and carbonyl groups, respectively. Chemical formulas detected here and in atmospheric chemistry studies
141 were compiled and tentatively used to evaluate the importance of autoxidation routes under both conditions.

142 **2 Experiments**

143 **2.1 Oxidation experiments**

144 The present experiments were carried out in a fused silica jet-stirred reactor (JSR) setup presented earlier (Dagaut et
145 al., 1986;Dagaut et al., 1988) and used in previous studies (Dagaut et al., 1987;Benoit et al., 2021;Belhadj et al.,
146 2021c). We studied separately the oxidation of the two isomers, α -pinene and limonene. As in earlier works (Benoit
147 et al., 2021;Belhadj et al., 2021c), α -pinene (+), 98% pure from Sigma Aldrich and limonene (R)-(+), >97% pure from

148 Sigma Aldrich, were pumped by an HPLC pump (Shimadzu LC10 AD VP) with an online degasser (Shimadzu DGU-
149 20 A3) and sent to a vaporizer assembly where it was diluted by a nitrogen flow. Each terpene isomer and oxygen,
150 both diluted by N₂, were sent separately to a 42 mL JSR to avoid oxidation before reaching 4 injectors (nozzles of 1
151 mm I.D.) providing stirring. The flow rates of nitrogen and oxygen were controlled by mass flow meters. Good thermal
152 homogeneity along the vertical axis of the JSR was recorded (gradients of < 1 K/cm) by thermocouple measurements
153 (0.1 mm Pt-Pt/Rh-10% wires located inside a thin-wall silica tube). In order to observe the oxidation of these isomers,
154 which are not prone to strong self-ignition, the oxidation of 1% of these chemical compounds (C₁₀H₁₆) under fuel-lean
155 conditions (equivalence ratio 0.25, 56% O₂, 43% N₂), was carried out at 590 K, atmospheric pressure, and a residence
156 time of 2 s. Under these conditions, the oxidation of the two isomers is initiated by slow H-atom abstraction by
157 molecular oxygen (RH + O₂ → R[•] + HO₂[•]). The fuel radicals R[•] react rapidly with O₂ to form peroxy radicals which
158 undergo further oxidation, characteristic of autoxidation. Nevertheless, this autoxidation mechanism, although
159 predominant, is not exclusive and other oxidation mechanisms are possible (Belhadj et al., 2021b). In this case, there
160 may be a random overlap of chemical formulas. The autoxidation criteria (two chemical formulas separated by two
161 oxygen atoms) allows to limit or avoid these overlaps.

162 2.2 Chemical analyses

163 A 2 mm I.D. probe was used to collect samples. To measure low-temperature oxidation products ranging from early
164 oxidation steps to highly oxidized products, the samples were bubbled into cooled acetonitrile (UHPLC grade ≥99.9,
165 T= 0°C, 250 mL) for 90 min. The resulting solution was stored in a freezer at -15°C. The stability of the products was
166 verified. No detectable changes in the mass spectra were observed after more than one month which is consistent with
167 previous findings (Belhadj et al., 2021c).

168 Analyses of samples collected in acetonitrile (ACN) were carried out via direct infusion (rate: 3 μL/min and recorded
169 for 1 min for data averaging) in the ionization chamber of a high-resolution mass spectrometer (Thermo Scientific
170 Orbitrap® Q-Exactive, mass resolution 140,000 and mass accuracy <0.5 ppm RMS). UHPLC conditions were: a
171 Vanquish UHPLC Thermo Fisher Scientific with a C18 column (Phenomenex Luna, 1.6 μm, 110 Å, 100x2.1 mm).
172 The column temperature was maintained at 40°C. 3 μml of sample were eluted by a mobile phase containing water-
173 ACN mix (pure water, ACN HPLC grade) at a flow rate of 250 μL/min (gradient: 5% to 20% ACN -3 min, 20% to
174 65% ACN - 22 min, 65% to 75% ACN - 4 min, 75% to 90% ACN - 4 min, for a total of 33 min).

175 Both heated electrospray ionization (HESI) and atmospheric chemical ionization (APCI) were used in positive and
176 negative modes for the ionization of products. HESI settings were: spray voltage 3.8 kV, vaporizer temperature of
177 150°C, capillary temperature 200°C, sheath gas flow of 8 arbitrary units (a.u.), auxiliary gas flow of 1 a.u., sweep gas
178 flow of 0 a.u.. In APCI, settings were: corona discharge current of 3 μA, spray voltage 3.8 kV, vaporizer temperature
179 of 150°C, capillary temperature of 200°C, sheath gas flow of 8 a.u., auxiliary gas flow of 1 a.u., sweep gas flow of 0
180 a.u.. In order to avoid transmission and detection effects of ions depending on their mass inside the C-Trap (Hecht
181 et al., 2019), acquisitions with three mass ranges were performed (m/z 50-750; m/z 150-750; m/z 300-750). The upper
182 limit of m/z 750 was chosen because of the absence of a signal beyond this value. It was shown that no significant
183 oxidation occurred in the HESI and APCI ion sources by injecting a limonene-ACN mixture (Fig. S1). The
184 optimization of the Orbitrap ionization parameters in HESI and APCI did not show any clustering phenomenon for
185 these two monoterpene isomers. The parameters evaluated were: injection source - capillary distance, vaporization

186 and capillary temperatures, applied difference of potential, injected volume, flow rate of nitrogen in the ionization
187 source. Positive and negative HESI mass calibrations were performed using PierceTM calibration mixtures (Thermo
188 Scientific). Chemical compounds with relative intensity less than 1 ppm to the highest MS signal in the mass spectrum
189 were not considered. Nevertheless, it should be considered that some of the molecules presented in this study could
190 result from our experimental conditions (continuous flow reactor, reagent concentration, temperature, reaction time)
191 and to some extent from our acquisition conditions, different from those in the previous studies (Deng et al.,
192 2021;Quéléver et al., 2019;Meusinger et al., 2017;Krechmer et al., 2016;Tomaz et al., 2021;Fang et al.,
193 2017;Witkowski and Gierczak, 2017;Jokinen et al., 2015;Nørgaard et al., 2013;Bateman et al., 2009;Walser et al.,
194 2008;Warscheid and Hoffmann, 2001;Hammes et al., 2019;Kundu et al., 2012). Operating with a continuous flow
195 reactor at elevated temperature and high initial concentration of reagents allows the formation of combustion-relevant
196 products, which does not exclude their possible formation under atmospheric conditions. To assess the formation of
197 products containing OOH and C=O groups, as in previous works (Belhadj et al., 2021a;Belhadj et al., 2021b), H/D
198 exchange with D₂O and 2,4-dinitrophenyl hydrazine derivation were used, respectively.

199 **3 Data Processing**

200 High resolution mass spectrometry (HR-MS) generates large datasets which are difficult to fully analyze by sequential
201 methods. When the study requires the processing of several thousands of molecules, the use of statistical tools and
202 graphical representation means becomes necessary. In this study, we have chosen to use the van Krevelen diagram
203 (Van Krevelen, 1950) by adding an additional dimension, the double bond equivalent (DBE). The DBE number
204 represents the sum of unsaturation and rings present in a chemical compound (Melendez-Perez et al., 2016). The
205 interest of this type of representation is to be able to identify more easily the clusters (increase of the DBE number at
206 constant O/C and H/C ratios)

$$207 \quad \text{DBE} = 1 + \text{C} - \text{H}/2$$

208 This number is independent of the number of O-atoms, but changes with the number of hydrogen atoms. Decimal
209 values of this number, which correspond to an odd number of hydrogen atoms, were not considered in this study. Then,
210 the superpositions of points (and therefore of chemical formulas) in the O/C vs. H/C space are suppressed. The
211 oxidation state of carbon (OSc) provides a measure of the degree of oxidation of chemical compounds (Kroll et al.,
212 2011). This provides a framework for describing the chemistry of organic species. It is defined by the following
213 equation:

$$214 \quad \text{OSc} \approx 2 \text{O/C} - \text{H/C}$$

215 **4 Results and discussion**

216 We studied the oxidation of α -pinene and limonene (C₁₀H₁₆) at 590 K, under atmospheric pressure, with a residence
217 time of 2 s, and a fuel concentration of 1%. Under these conditions, the formation of peroxides by autoxidation at low
218 temperature should be efficient (Belhadj et al., 2021c), even though the conversion of the fuels remains moderate.

219 4.1 Characterization of ionization sources

220 First, we have studied the impact of APCI and HESI sources, in positive and negative modes, on the chemical formulas
 221 detected. The HESI and APCI sources in positive and negative mode were used and their operating parameters were
 222 varied, i.e., temperature, gas flow and accelerating voltage (see Section 2). For each polarity, only ions composed of
 223 carbon, hydrogen (even numbers) and oxygen were considered. Molecular duplicates inherent to mass range overlaps
 224 were excluded. By following these rules, we obtained a different number of ions depending on the ionization source
 225 and the polarity used. Table 1 shows the number of ions according to the experimental conditions and the
 226 discrimination rules.

227 **Table 1.** Number of ions detected for each source in positive and negative modes (by protonation or deprotonation,
 228 respectively)

Ionization source	α -Pinene		Limonene	
APCI	646 (R+H) ⁺	503 (R-H) ⁻	1321 (R+H) ⁺	1346 (R-H) ⁻
HESI	594 (R+H) ⁺	693 (R-H) ⁻	1017 (R+H) ⁺	1864 (R-H) ⁻

229

230 Each combination of ionization sources and polarity generated a set of chemical formulas. To make a meaningful
 231 comparison between the positive and negative ions data, the chemical formulas used were the precursors of the ions
 232 identified in the mass spectra. These sets have common data, but also specific chemical formulas. For a given
 233 ionization source, ~ 50% of the chemical formulas are observed whatever the ionization polarity, i.e., using both
 234 polarities one can capture between 30-50% more molecular species (since some of them are ionized under a single
 235 mode (+ or -) depending on their chemical structure). Utilizing both ionization polarities is helpful for identifying a
 236 larger quantity of species. The HESI source data were compared to the APCI data (Supplement, Tables S1 and S2),
 237 showing an increased number (20 to 30%) of chemical formulas detected by HESI. This increase is characterized by
 238 a better detection of negatively ionized species and those with a higher DBE. In order to evaluate further the interest
 239 for using these ionization sources, we compiled these data in Venn diagrams and proposed a visualization of these sets
 240 with a van Krevelen representation; we added the number of DBE in the third dimension (Supplement, Tables S1 and
 241 S2).

242 In positive ionization mode, independently of the ionization source and in addition to the common molecular formulas,
 243 we detected products with an O/C ratio < 0.2 whereas in the negative ionization mode, we detected molecular formulas
 244 with an O/C ratio > 0.5. In addition to these observations, we noted that HESI is more appropriate for studying products
 245 with a large number of unsaturation (DBE > 5), which is probably related to the increase in the number of
 246 hydroperoxide and carboxyl groups along with the fact that a heated ionization source favors vaporization of low
 247 volatility compounds. Finally, for an optimal detection of the oxidation products, it is necessary to consider the
 248 transmission limits of the C-Trap. Here, we could increase by more than 60% the number of molecular formulas
 249 detected using several mass ranges for data acquisition (section 2.2). The most appropriate ionization polarity to be
 250 used is tied to chemical functions present in products to be detected. We could increase by 30 to 100% the number of
 251 chemical formulas detected by using both positive and negative ionization modes. Using HESI is consistent with
 252 previous findings indicating ESI is well suited for the ionization of acidic, polar, and heteroatom-containing chemicals
 253 (Kekäläinen et al., 2013). To illustrate the present results, HESI (-)-MS spectra are provided in the Supplement (Fig.

254 S2). The list of all chemical formulas found in limonene and α -pinene samples (HESI negative and positive mode) is
255 given in the data-supplement file

256

257 4.2 Autoxidation products detected in a JSR

258 In order to compare the oxidation of α -pinene and limonene, we compiled the positive and negative ionization data
259 obtained with APCI (Table S1) and HESI (Table S2) ionization sources to obtain a more exhaustive database. For the
260 APCI and HESI sources, we distinguished three datasets, two of which are specific to the oxidation of α -pinene and
261 limonene and one which is common to both isomers. In the following text, "only" will be used to describe the
262 molecules specific to the oxidation of one of the isomeric terpenes. This common dataset represents more than 77.90%
263 of the chemical formulas identified in the α -pinene oxidation samples detected with APCI or HESI. For limonene, for
264 which the number of identified chemical formulas is greater/larger, regardless of the ionization source, this common
265 dataset/data set represents over 93/nearly 40% of the chemical formulas detected after APCI ionization. In these two
266 cases, the relatively low residence time (2 seconds) and the diversity of the chemical formulas obtained suggest that
267 the oxidation of these two terpene isomers leads to ring opening, a phenomenon also observed in atmospheric
268 chemistry (Berndt et al., 2016;Zhao et al., 2018;Iyer et al., 2021). Concerning the molecular formulas of products
269 common to both isomers, Figure 1 shows that they are limited to compounds with 10 oxygen atoms or lower. This
270 limit is linked to α -pinene whose oxidation beyond 10 oxygen atoms remains weak (less than 2% of the detected
271 molecules for this terpene). In the case of limonene, the presence of an exocyclic double bond will increase, in a similar
272 way to atmospheric chemistry (Kundu et al., 2012), the possibilities of oxidation and accretion. It remains however
273 impossible, considering the size of the whole dataset and the diversity of the isomers, to formalize all the reaction
274 mechanisms. Nevertheless, the formation of oxidized species can be described with the help of graphical tools. The
275 number of oxygen atoms per molecule indicates that limonene oxidizes more than α -pinene (Fig. 1a). In the case of
276 limonene, with a HESI source, chemicals with an oxygen number of up to 15 were detected. Most of the chemical
277 formulas recorded had 8-10 O-atoms (Fig. 1c), whereas for α -pinene the products with >8 O-atoms were much less
278 abundant (Fig. 1b). Moreover, for the products specific of limonene oxidation, this graph shows a distribution centered
279 on 9 oxygen atoms with carbon skeletons probably resulting from accretion.

280

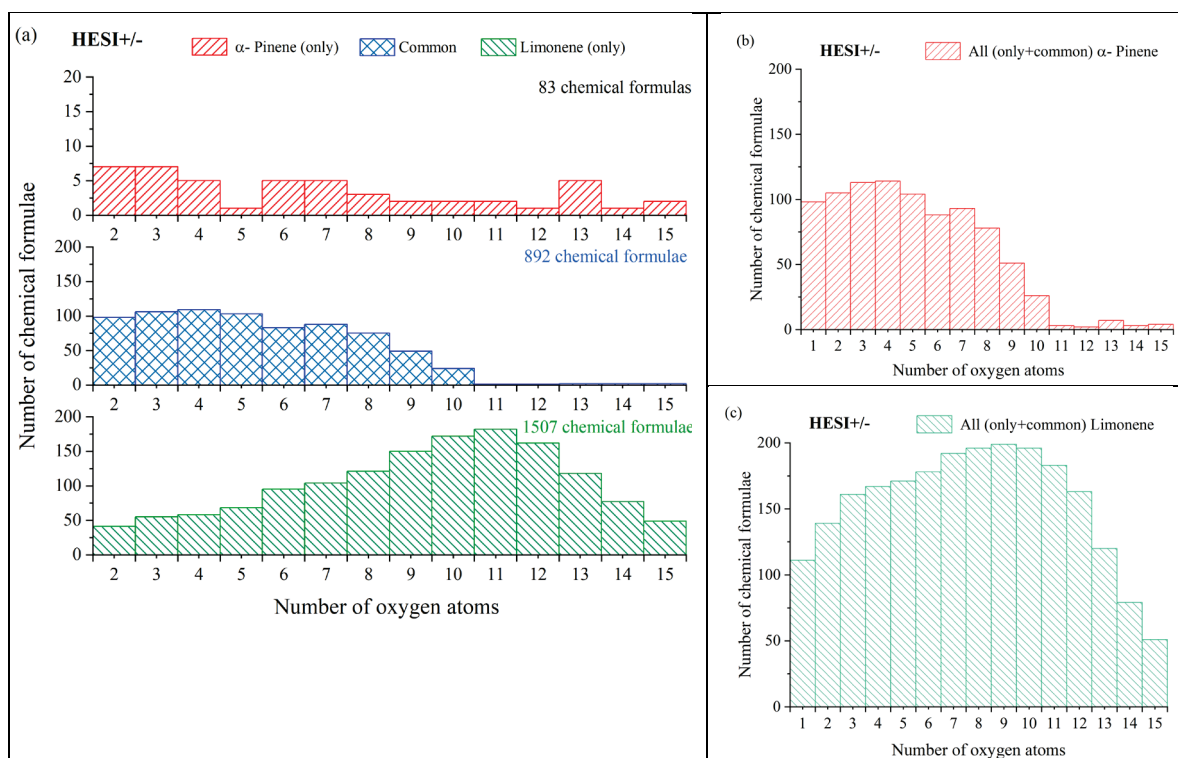
281

282

283

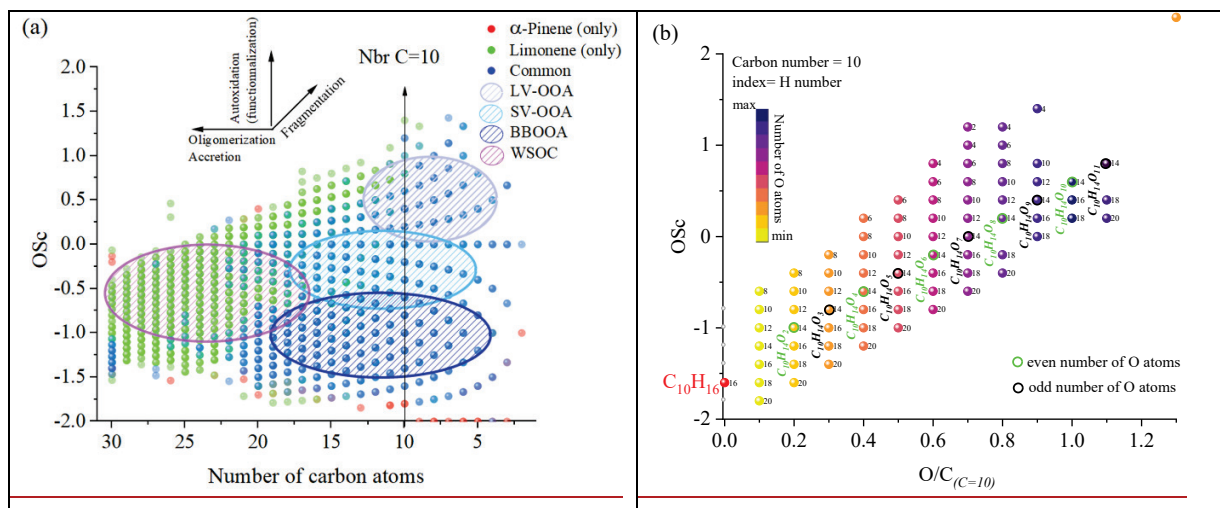
284

285



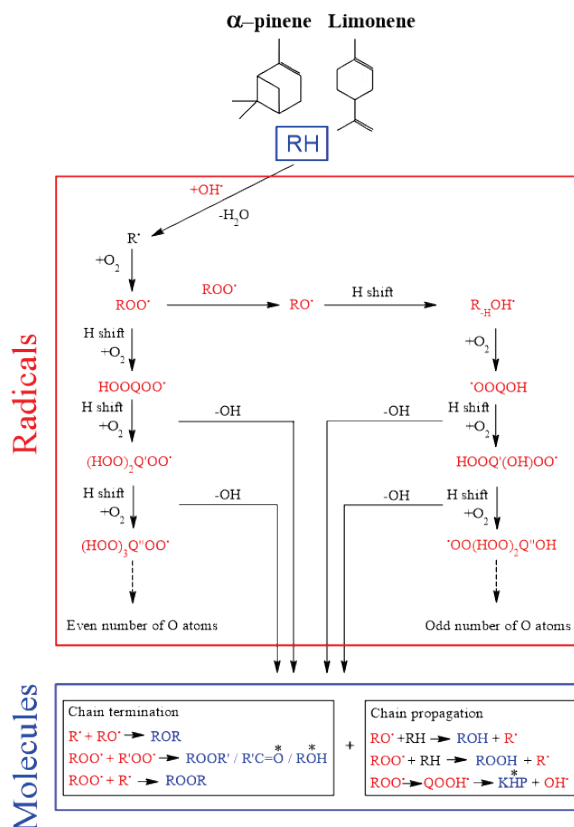
286
 287 **Figure 1:** Distribution of α -pinene and limonene ~~autoxidation~~oxidation products as a function of their oxygen content
 288 (ionization source: HESI, combined positive and negative modes data). (a) α -pinene and limonene HESI(+/-), (+/-),
 289 (b) α -pinene HESI(+/-), (c) limonene HESI(+/-)

290 To verify this accretion hypothesis, we can plot the OSc as a function of the number of carbon atoms or the O/C ratio
 291 at fixed number of C-atoms (Fig. 2). Indeed, the presence of chemical compounds with 11 carbon atoms can be
 292 explained by an accretion phenomenon (Wang et al., 2021), but the advantage of this OSc vs. nC space representation
 293 (Kroll et al., 2011) is to allow studying this phenomenon on all the data. One can visualize the evolution of the
 294 molecular oxidation for each carbon skeleton and the formation of oligomers. Species that are unique to one of the
 295 isomers, or common to both are differentiated using different colors. In addition ~~to the autoxidation represented by the~~
 296 ~~vertical axis for a given number of carbon atoms (, in Fig. 2a),~~ we observe mechanisms of fragmentation ($C_{<10}$),
 297 accretion and oligomerization ($C_{>10}$). These reaction mechanisms contribute to forming chemical classes according to
 298 their number of carbon atoms, up to $C=30$. This limit is probably due to the ionization or detection capacity of the
 299 spectrometer. The increase in the number of oxygen atoms, but also of carbon atoms will decrease products volatility.
 300 Following a classification proposed in the literature (Kroll et al., 2011), we distinguished four sets of products: low
 301 volatile oxidized organic aerosols (LV-OOA), semi-volatile oxidized organic aerosols (SV-OOA), biomass burning
 302 organic aerosols (BBOA) and water-soluble organic carbons (WSOC). In the OSc versus carbon number plot (Fig 2a),
 303 the vertical lines (at constant carbon number) are a first criterion for finding potential candidate products of
 304 autoxidation. Figure 2b shows, for a fixed number of carbon and hydrogen atoms ~~and a difference,~~ the diversity of
 305 ~~two oxidized species formed. Different~~ oxygen ~~atoms, the potential~~ parities are observed, showing that different
 306 reaction mechanisms occur.



307 **Figure 2.** Overview of the distribution of limonene and α -pinene oxidation products of autoxidation connected by
 308 arrows whose color characterizes the oxygen parity. We can measure the extent of autoxidation for each carbon
 309 backbone observed in the JSR: (a) OSc vs. O/C space. Using these criteria, we found that 73% of all versus carbon
 310 number in detected chemical formulas are linked by a single difference of two oxygen atoms (which reflects an
 311 autoxidation mechanism). For the two terpenes, for which the initial from APCI and HESI data. (b) Molecular
 312 formulas detected in this study presented in the OSc versus O/C space for a carbon number is equal to 10, one can
 313 observe (Fig. 2b) two autoxidation routes with an even and odd of 10; index of the products: number of
 314 oxygen/hydrogen atoms, respectively.

315 This parity distinction is initially present for the two main radicals, ROO \cdot and RO \cdot involved in autoxidation
 316 mechanisms. However, termination and propagation reactions will change the oxygen parity (Fig. 3). Then, parity
 317 links between radicals and molecules are lost, which prevents interpretation of radical oxidation routes (Fig. 3). Figure
 318 3 illustrates one of the reaction mechanisms (OH oxidation pathway) where oxygen parity changes through
 319 autoxidation. It should be noted that other reaction mechanisms can also change oxygen parity. In addition, the OH
 320 pathway in ozonolysis is not predominant. Figure 2 (b) illustrates the autoxidation routes between molecules resulting
 321 from a hydroperoxy radical reaction (arrows). In this case the oxygen parity is not modified and an OH radical is
 322 formed. HESI data showed an equivalent distribution of oxygen parities in molecular products (odd: 51%, even 49%)
 323 therefore confirming a lack of selectivity of the reaction mechanisms with respect to the oxygen parity of
 324 radicals which cannot allow concluding on the relative importance of reaction pathways. It should be noted that other
 325 reaction mechanisms can also change oxygen parity, e.g., QOOH \rightarrow cyclic ether (QO) + OH (Wang et al., 2017).
 326 Figure 2 (b) illustrates the autoxidation products presented in Fig. S3. There, one can see the formation routes to even-
 327 oxygen compounds $C_{10}H_{14}O_{2 \text{ to } 10}$ and to odd-oxygen compounds $C_{10}H_{14}O_{3 \text{ to } 11}$. The molecular formulas detected in
 328 our experiments as shown in bold in Fig. 2b. The others formulas presented in Fig. 2b should result from others
 329 oxidation pathways. Indeed, products with chemical formulas with $H \geq 16$ cannot derive from the autoxidation
 330 pathways described in Fig S3. Other pathways (Fig. S5) can yield such species, e.g., through the initial addition of OH
 331 on terpenes double bonds followed by O_2 addition and autoxidation of resulting products.



332
 333 **Figure 3.** Accepted autoxidation reaction mechanisms in combustion (left) and in the atmosphere (left and right). *
 334 indicates a change of oxygen atoms parity (Berndt et al., 2016).

335 Nevertheless, despite this change in parity, in the case of autoxidation, the free-radical reaction pathway (shown in
 336 Supplements Figs. S3 and S5 for both oxygen parities) can produce a set of molecular products that mirrors repeated
 337 O₂ addition, characteristic of autoxidation (Fig. 2b). Furthermore, we studied the relative intensities of identified
 338 chemical formulas for alpha pinene and limonene (HESI source). The results presented in Table 2 show overall a
 339 decrease in relative intensities of products signal with increasing number of oxygen atoms (C₁₀H₁₄O_{2,4,6,8...};
 340 C₁₀H₁₄O_{3,5,7...}) for both terpenes. It is clear that the repeated addition of O₂ on radicals (Fig S3) associated with the
 341 decrease of the relative intensities of the products formed is not sufficient to assess an autoxidation mechanism
 342 although it is a necessary step to constrain the identification phase of the isomers, otherwise impossible within sets
 343 composed of several thousands of chemical molecules. Finally, few chemical formulas with no chemical relevance
 344 (C_xH₄O_y) were detected. These are probably artefacts linked to the characterization method (ionization mode, ions
 345 transfer, ions isolation in the C-trap, incorrect masse identification). We chose to leave these data, knowing that they
 346 would be discarded in the various subsequent comparisons.

347

348

349

350

351

352

353

354

355

Table 2: Relative intensities of detected chemical formulas for alpha pinene and limonene (HESI– data) which could result from autoxidation of these terpenes. Signal intensities are given in parentheses. Chemical formulas are highlighted in red in the Supplementary database.

	Limonene	Alpha-pinene
Even number of oxygen atom		
hydroxyketone	<u>C₁₀H₁₄O₂ (1.61442E+7)</u>	<u>C₁₀H₁₄O₂ (4.54785E+7)</u>
+O₂ (1st)	<u>C₁₀H₁₄O₄ (3.34718E+7)</u>	<u>C₁₀H₁₄O₄ (2.52885E+6)</u>
+O₂ (2nd)	<u>C₁₀H₁₄O₆ (9.58108E+6)</u>	<u>C₁₀H₁₄O₆ (7.56393E+4)</u>
+O₂ (3rd)	<u>C₁₀H₁₄O₈ (9.55306E+5)</u>	<u>C₁₀H₁₄O₈ (2.91182E+4)</u>
+O₂ (4th)	<u>C₁₀H₁₄O₁₀ (1.00597E+4)</u>	<u>C₁₀H₁₄O₁₀ (not detected)</u>
	<u>C₁₀H₁₄O₁₂ (not detected)</u>	==
Odd number of oxygen atom		
hydroperoxy carbonyl	<u>C₁₀H₁₄O₃ (3.23297E+7)</u>	<u>C₁₀H₁₄O₃ (9.3999E+6)</u>
+O₂ (1st)	<u>C₁₀H₁₄O₅ (2.27278E+7)</u>	<u>C₁₀H₁₄O₅ (1.17044E+5)</u>
+O₂ (2nd)	<u>C₁₀H₁₄O₇ (4.04207E+6)</u>	<u>C₁₀H₁₄O₇ (7.17307E+4)</u>
+O₂ (3rd)	<u>C₁₀H₁₄O₉ (1.92816E+5)</u>	<u>C₁₀H₁₄O₉ (not detected)</u>
+O₂ (4th)	<u>C₁₀H₁₄O₁₁ (6.34129E+3)</u>	==
	<u>C₁₀H₁₄O₁₃ (not detected)</u>	==

356

357 4.3 Combustion versus atmospheric oxidation

358 4.3.1 Global analysis

359 We have explored potential chemical pathways related to autoxidation in the previous Section. For this purpose, we
 360 have performed experiments under cool flame conditions (590 K). This autoxidation mechanism is also present in
 361 atmospheric chemistry, but it is only recently that it has been found that this mechanism could be one of the main
 362 formation pathways for SOA (Savee et al., 2015; Crounse et al., 2013; Jokinen et al., 2014a; Iyer et al., 2021). Studies
 363 have described this mechanism in the case of atmospheric chemistry with the identification of radicals and molecular
 364 species (Tomaz et al., 2021). However, previous studies on the propagation of this reaction mechanism have mainly
 365 focused on the initial steps of autoxidation without screening all identified chemical formulas for potential autoxidation
 366 products. It is therefore useful to assess the proportion of possible autoxidation products among the total chemical
 367 species formed.

368 Here, we propose a new approach which consists in assessing a set of molecules mainly resulting from autoxidation
 369 against different sets of experimental studies related to atmospheric chemistry. The objective is to evaluate similarity
 370 of oxidation products formed under these conditions. For this purpose, we selected a HESI ionization source, better
 371 suited for detecting higher polarity oxidized molecules, as well as higher molecular weight products (detection of 96%
 372 of the total chemical formulas observed in autoxidation by APCI and HESI).

373 Among published atmospheric chemistry studies of terpenes oxidation, we have selected 15 studies presenting enough
 374 chemical products of oxidation, 4 for α -pinene and 11 for limonene. The data were acquired using different

375 experimental procedures (methods of oxidation, techniques of characterization). Table 23 summarizes all the
376 experimental parameters related to the selected studies. From that Table, one can note that few studies involved
377 chromatographic analyzes (Tomaz, 2021; Witkowski and Gierczak, 2017; Warscheid and Hoffmann, 2001). The data
378 are from the articles or files provided in the Supplement Tables S1 and S2. In these studies, oxidation was performed
379 only by ozonolysis with different experimental conditions that gather the main methods described in the literature:
380 ozonolysis, dark ozonolysis, ozonolysis with OH scavenger, ozonolysis with or without seed particles. We considered
381 that the ~~ionisation~~ionization mode used in mass spectrometry did not modify the nature of the chemical species but
382 only the relative detection of ions, depending on the type of ionization used, and the sensitivity of the instruments
383 (Riva et al., 2019). The combination of data obtained using ~~(+/-)~~(+/-) HESI gives a rather complete picture of the
384 autoxidation products.

385 First, we compared the data from ozonolysis studies of each terpene and identified similarities through Venn diagrams.
386 For studies with two ionization sources, duplicate chemical formulas were removed. We selected the four most
387 representative studies by the number of the chemical formulas detected. Then, we compared the set of chemical
388 formulas identified after ozonolysis to those produced in low-temperature combustion, the objective being (i) to
389 highlight similarities in terms of products generated by the two oxidation modes and (ii) to identify chemicals resulting
390 from autoxidation.

391

392

393 **Table 23.** Experimental settings of 15 oxidation studies of two terpenes under atmospheric conditions and cool
 394 flames (LC stands for liquid chromatography).

Reference	Oxidation mode	Sampling	Experimental setup	Concentrations of reactants	Ionization /source	Instrument	Chemical formulas	LC
α-Pinene								
Y. Deng et al. (2021)	Dark ozonolysis seed particles OH scavenger	online	Teflon bag; 0.7m ³	3.3±0.6 ncps ppbv ⁻¹ α -Pinene	ESI	ToF-MS	351	No
Quéléver et al. (2019)	Ozonolysis	online	Teflon bag 5 m ³	10 & 50 ppb α -Pinene	NO ₃ ⁻ (CI)	CI-API-TOF	68	No
Meusinger et al. (2017)	Dark Ozonolysis OH scavenger no seed particles	offline	Teflon bag 4.5 m ³	60 ppb α -Pinene	Proton transfer	PTR-MS-ToF	153	No
Krechmer et al. (2016)	Ozonolysis	offline	PAM Oxidation reactor	Field measurement	ESI (-) and NO ₃ ⁻ (CI)	CI-IMS-ToF	43	No
This work	Cool-flame autoxidation	offline	Jet-stirred reactor 42 ml	1%, α -pinene No ozone	APCI(3kV) HESI (3kV)	Orbitrap® Q-Exactive	820 (APCI) 975 (HESI)	Yes
Limonene								
Krechmer et al. (2016)	Ozonolysis	offline	PAM Oxidation reactor	not specified	ESI (-) and NO ₃ ⁻ (CI)	CI-IMS-ToF	63	No
Tomaz et al. (2021)	Ozonolysis	online	Flow tube reactor (18L)	45-227 ppb limonene	NO ₃ ⁻ (CI) - Neg	Orbitrap® Q-Exactive	199	Yes
Fang et al. (2017)	OH-initiated photooxidation dark ozonolysis	online	Smog chamber	900–1500 ppb limonene	UV; 10 eV	Time-of-Flight (ToF)	17	No
Witkowski and Gierczak (2017)	Dark ozonolysis	offline	Flow reactor	2 ppm, limonene	ESI, 4.5 kV	Triple quadrupole	12	Yes
(Jokinen et al., 2015)	Ozonolysis	online	Flow glass tube	1–10000 x10 ⁹ molec.cm ⁻³ , limonene	NO ₃ ⁻ (CI)	Time-of-Flight (ToF)	11	No
Nørgaard et al. (2013)	Ozone (plasma)	online	direct on the support	850 ppb ozone 15-150 ppb limonene	plasma	Quadrupole time-of-flight (QToF)	29	No
Bateman et al. (2009)	Dark and UV radiations ozonolysis	offline	Teflon FEP reaction chamber	1 ppm ozone 1 ppm limonene	modified ESI (+/-)	LTQ-Orbitrap Hybrid Mass (ESI)	924	No
Walser et al. (2008)	Dark ozonolysis	offline	Teflon FEP reaction chamber	1-10 ppm ozone 10 ppm limonene	ESI (+/-); 4.5 kV	LTQ-Orbitrap Hybrid Mass (ESI)	465	No
Warscheid & Hoffmann (2001)	Ozonolysis	online	Smog chamber	300-500 ppb limonene	APCI; 3kV	Quadrupole ion trap mass	21	Yes
Hammes et al., (2019)	Dark ozonolysis	online	Flow reactor	15, 40, 150 ppb limonene	²¹⁰ Po α acetate ions	HR-ToF-CIMS	20	No
Kundu et al. (2012)	Dark ozonolysis	offline	Teflon reaction chamber	250 ppb ozone 500 ppb limonene	ESI; 3.7 and 4 kV	LTQ FT Ultra, Thermo Sct (ESI)	1197	No
This work	Cool-flame autoxidation	offline	Jet-stirred reactor 42 ml	1%, limonene No ozone	APCI(3 μ A) HESI (3kV)	Orbitrap® Q-Exactive	1863(APCI) 2399(HESI)	Yes

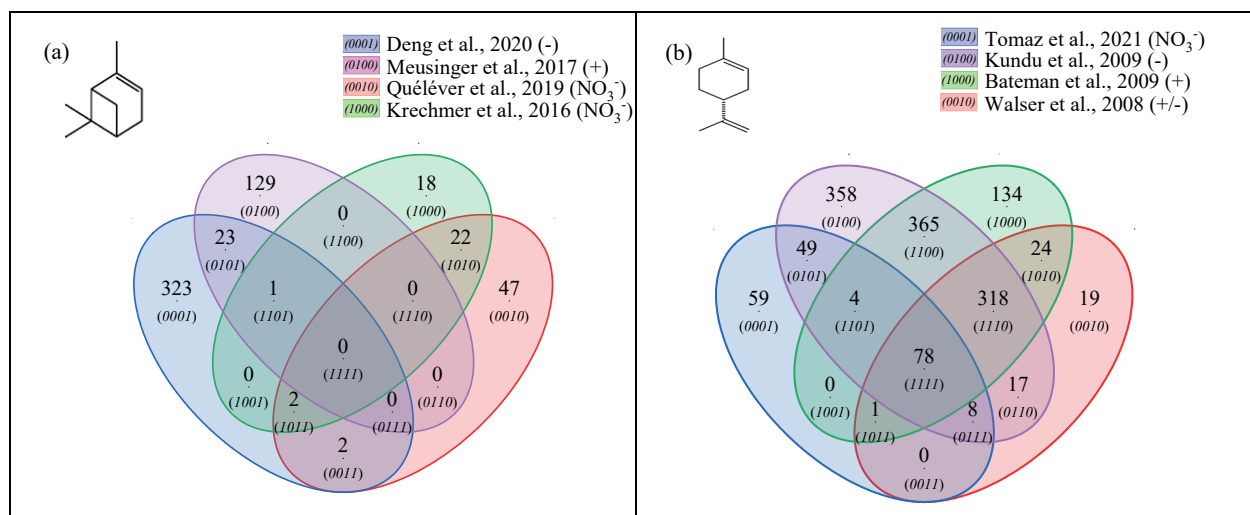
395

396 For α -pinene oxidation, in the four selected studies 567 chemical formulas were detected, all polarities combined.

397 Only one study (Meusinger et al., 2017) was performed in positive ionization mode and none of the studies reported

398 data were obtained with two ionization modes (+/-). For the oxidation of limonene, the four selected studies identified
 399 1434 chemical formulas. Among these studies, the experiments by Walser et al. were performed with both (+) and (-
 400) ~~ionisation~~ ionization modes. In contrast to the α -pinene case, the selected studies for limonene were performed with
 401 similar ionization sources, which probably contributed to increased data similarity (Walser et al., 2008). In the case of
 402 limonene oxidation, for which accretion is more important than for α -pinene, and for which a greater number of
 403 chemical formulas were identified, the similarities are more important (Jokinen et al., 2014b). These results are
 404 presented in Figure 4 where the ionization polarity used in each study is specified.

405



406 **Figure 4:** Venn diagrams for comparing the oxidation results from ozonolysis of (a) α -pinene and (b) limonene (see
 407 conditions in Table 1). Each digit indicates a study, the value of the digit characterizes the presence (value 1) or
 408 absence (0) common products detected in different studies, e.g., 23 chemical formulas (0101) (Fig. 4a) are common
 409 to the studies of Deng et al; (0001) and Meusinger et al. (0100)

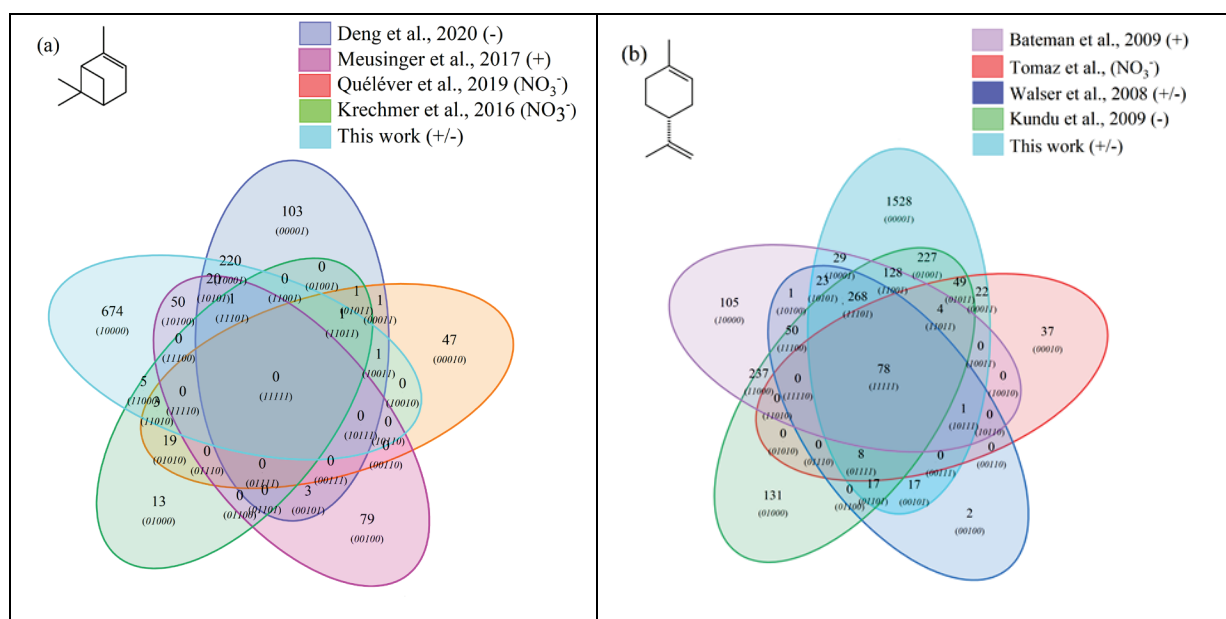
410 For α -pinene, no chemical formula is common to all datasets. Different hypotheses can be offered to explain this
 411 result. Among them, the number of chemical formulas identified per study remains limited (a few dozen to several
 412 hundred) and these small datasets are sometimes restricted to specific mass ranges, e.g. C₁₀ to C₂₀ (Quéléver et al.,
 413 2019). In the case of studies carried out with an NO₃⁻ source, sensitive to HOMS, produced preferentially by
 414 autoxidation, we note that nearly 50% of the chemical formulas (10/22; (1010)) are linked by a simple difference of 2
 415 oxygen atoms.

416 For limonene, ~~78~~ 78 chemical formulas are common to the four studies selected here. In this data set, a large majority of
 417 chemical formulas show a similar relationship to autoxidation, i.e., a simple difference of two oxygen atoms: 62%
 418 (Tomaz et al., 2021), 54% (Walser et al., 2008), 69% (Kundu et al., 2012), 66% (Bateman et al., 2009) and 72% (this
 419 study). This result seems to indicate that autoxidation dominates.

420 One can then ask if reaction mechanisms common to atmospheric and combustion chemistry can generate, despite of
 421 radically different experimental conditions, a set of common chemical formulas and if in this common dataset, a
 422 common link, characteristic of autoxidation, is observable? To address that question, we compared all the previous
 423 results, for each of these terpenes to those obtained under the present combustion study. The comparisons were made
 424 using our HESI data. One should remember that the oxidation conditions in the JSR were chosen in order to maximize
 425 low-temperature autoxidation. Again, we used Venn diagrams to analyze these datasets consisting of 1590 chemical

426 formulas in the case of α -pinene and 5184 chemical formulas in the case of limonene. The results of these analyses
 427 are presented in Figure 5.

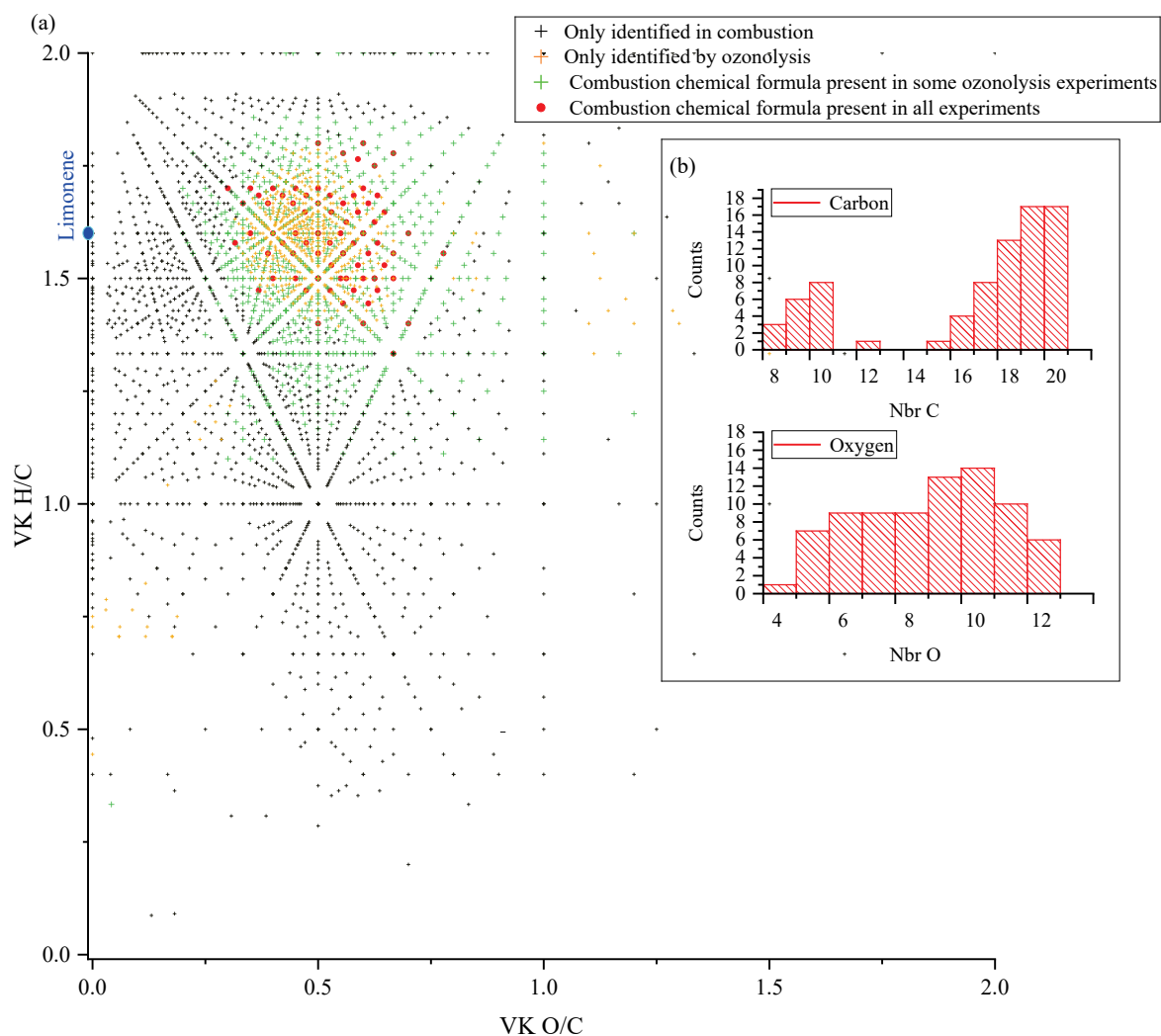
428 It turned out that for α -pinene, 301 chemical formulas and for limonene 871 chemical formulas were common to
 429 oxidation by ozonolysis (with or without scavenger) and combustion. This represents 31% of the chemical formulas
 430 for the ozonolysis of α -pinene and 36% for those of limonene ozonolysis. For α -pinene, the similarities compared to
 431 combustion are specific to each study: (Deng et al., 2021) 69% (243), (Meusinger et al., 2017) 46%, (71) (Quéléver et
 432 al., 2019) 7% (5), (Krechmer et al., 2016) 23% (10). Chemical formulas common to all studies were not identified.
 433 This lack of similarity may be due to a partial characterization of the chemical formulas, a weaker oxidation of α -
 434 pinene with an ionization mode less favorable to low molecular weights products.



435 **Figure 5:** Venn diagrams comparing the oxidation results from ozonolysis and combustion of (a) α -pinene and (b)
 436 limonene (see conditions in Table 1).

437 For limonene, the similarities with combustion are more important and less spread out. They represent for the different
 438 studies: 65% (Kundu et al., 2012), 88% (Walser et al., 2008), 81% (Tomaz et al., 2021), and 57% (Bateman et al.,
 439 2009). Moreover, there is a common dataset of 78 chemical formulas which can derive from autoxidation mechanisms.
 440 Considering the very different experimental conditions, we must wonder about the impact of the double bonds in this
 441 similarity. In the case of limonene, we think their presence will indeed promote the formation of allylic radicals and
 442 then peroxide radicals (one of the motors of autoxidation). It is necessary to specify again that different reaction
 443 mechanisms can cause the observed similarities. However, the preponderance of autoxidation in so-called cool flame
 444 combustion is obvious, and in atmospheric chemistry, this reaction mechanism is competitive or dominates (Crouse
 445 et al., 2013; Jokinen et al., 2014a). If we search for an autoxidation link between these 78 chemical formulas, we
 446 observe that 45% of these chemical formulas meet this condition: difference of two oxygen atoms between formulas,
 447 at constant number of carbon and hydrogen atoms. [\(Data supplements, tab-5\)](#) More precisely, these molecules are
 448 centered in a van Krevelen diagram on the ratios $O/C=0.6$ and $H/C=1.6$, in the range $0.29 < O/C < 0.77$ and $1.33 <$
 449 $H/C < 1.8$. All oxidized molecules associated with this dataset are presented in Figure 6. The dispersion of the chemical
 450 ~~formulas~~ formulae, far from being random, ~~remains consistent~~ could be correlated with an autoxidation mechanism
 451 where the ~~numbers~~ number of carbon and hydrogen atoms are constant.

452



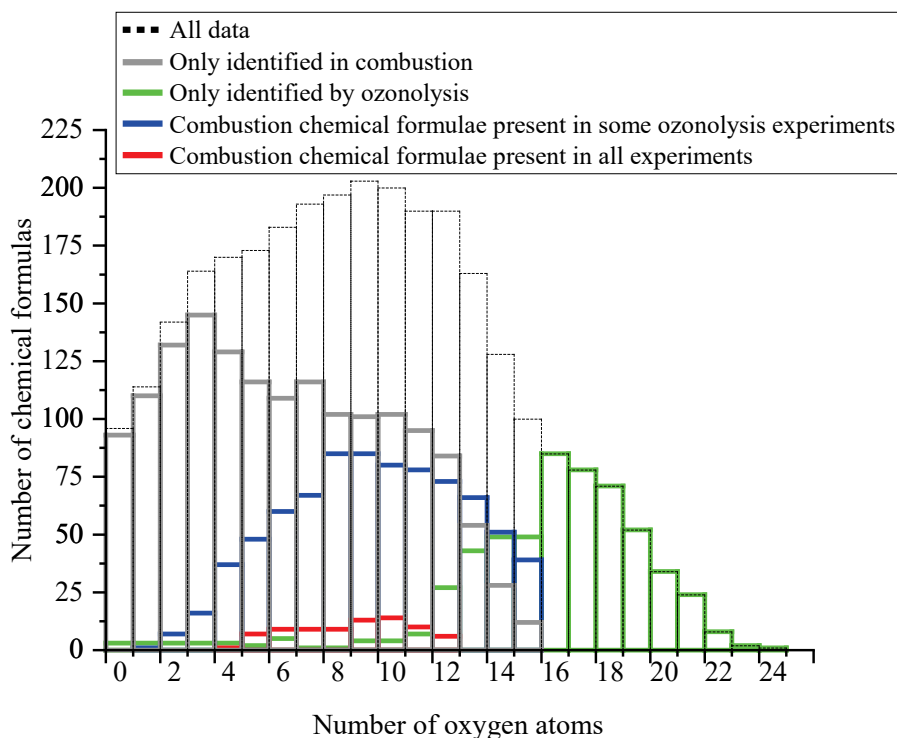
453

454 **Figure 6:** (a) Van Krevelen diagram showing specific and common chemical formulas detected after to oxidation of
 455 limonene by ozonolysis and combustion; insert (b): distributions of the number of carbon and oxygen atoms in the
 456 78 chemical formulas common to all experiments.

457 A 3-D representation of all limonene oxidation data is given in Supplement (Fig. [S3aS4a](#)) where DBE is used as third
 458 dimension. From that figure, one can note that products with higher DBE (DBE>10) are preferably formed under JSR
 459 conditions, i.e., at elevated temperature. A 2D representation (OSc vs DBE, Fig. [S3bS4b](#)) completes this 3D view.
 460 The corresponding chemical formulas with DBE > 10 could correspond to carbonyls and / or cyclic ethers (*QOOH
 461 → carbonyl + alkene + OH and / or cyclic ether + OH*). Specificities and similarities of these two oxidation modes
 462 (ozonolysis/combustion) were further investigated by plotting the distribution of the number of oxygen atoms in
 463 detected chemical formulas (Fig. 7). Indeed, the distribution of the number of oxygen atoms allows, in addition to the
 464 Van Krevelen diagram, to provide some additional details on these two modes of oxidation. In ozonolysis, we observed
 465 the chemical formulas having the largest number of oxygen atoms. There, oxidation proceeds over a long reaction
 466 time where the phenomenon of aging appears through accretion or oligomerization. In combustion, the number of
 467 oxygen atoms remains limited to 18, with a lower number of detected chemical formulas compared to the case of
 468 ozonolysis. However, JSR-FIA-HRMS data indicated many more sets of chemical formulas differing by two O-atoms

469 [in the range \$C_{10}H_xO_{2-10}\$ \(\$C_{10}H_{12}O_{2-10}\$, \$C_{10}H_{12}O_{3-9}\$, \$C_{10}H_{14}O_{2-10}\$, \$C_{10}H_{14}O_{3-9}\$, \$C_{10}H_{16}O_{2-8}\$, \$C_{10}H_{16}O_{3-9}\$ \); see Supplementary](#)
 470 [database, tab-4. Although at this stage one cannot prove these species were formed through autoxidation, their formulas](#)
 471 [are consistent with autoxidation products.](#) It is in combustion that we observed the highest O/C ratios, indicating the
 472 formation of the most oxidized products. This difference, however, does not affect the similarities between the
 473 chemical formulas detected in the two modes of oxidation. Finally, the analysis of the parities in oxygen atoms, very
 474 similar for the three datasets, confirms that the reaction mechanisms presented in Figure 3 do not allow a simple link
 475 to be established between the oxygen parity of radicals and that of the detected molecular products. [The list of these](#)
 476 [78 chemical formulas is given in the data-supplement file](#)

477



478

479 **Figure 7:** Oxygen number distribution for all the molecules identified for the oxidation of limonene: only in
 480 combustion, only in ozonolysis and common to both processes.

481 4.3.2 Identification of common isomers.

482 We identified a set of chemical formulas common to both atmospheric and combustion [chemistries/oxidation modes](#)
 483 and suggested that this might result from an autoxidation mechanism. We ~~identified~~[detected](#) several chemical formulas
 484 within this dataset that differ by two oxygen atoms on the same skeleton- ($C_{10}H_{16}O_x$). [Some of these chemical formulas](#)
 485 [were previously identified in Figure 2b or in the 78 common chemical formulas.](#) Focusing on the early stages of
 486 limonene oxidation, there are several ~~sequential two oxygen additions to the~~[chemical formulas, starting from](#)
 487 $C_{10}H_{16}O_2$ and $C_{10}H_{16}O_3$ ~~with the two oxygen parities described in Figure 3. Tables 3,~~ [which contain increasing \(by 2\)](#)
 488 [number of oxygen atoms. Table 4](#) presents the identified chemical formulas with ~~information on the~~[Venn index given](#)
 489 [in parentheses and ions intensity.](#) The index for combustion is the rightmost (xxxx1).

490 [Table 3. Sequential additions](#)4. [Products of two oxygens to the multiple addition of oxygen on limonene oxidation](#)
 491 [product by OH.](#) Chemical formulas $C_{10}H_{16}O_2$ and $C_{10}H_{16}O_3$ ~~present~~[are highlighted in the common set of 78 chemical](#)
 492 [formulas](#) ~~red~~[in the Supplementary database.](#)

First stages of oxidation	1st addition	2nd addition	3rd addition	4th addition	5th addition
C ₁₀ H ₁₆ O ₂ (10101) 3.64425E+6	C ₁₀ H ₁₆ O ₄ (11101) 1.01228E+7	C ₁₀ H ₁₆ O ₆ (11111) 1.99061E+6	C ₁₀ H ₁₆ O ₈ (01011) 8.62699E+4	C ₁₀ H ₁₆ O ₁₀ (00011) 4.33184E+4	C ₁₀ H ₁₆ O ₁₂ (00010)
C ₁₀ H ₁₆ O ₃ (11101) 1.2035E+7	C ₁₀ H ₁₆ O ₅ (11111) 5.91408E+6	C ₁₀ H ₁₆ O ₇ (11111) 4.90565E+5	C ₁₀ H ₁₆ O ₉ (01011) 2.08502E+4	C ₁₀ H ₁₆ O ₁₁ (00010)	

493
494 ~~This result~~A proposed formation route of sequential the C₁₀H₁₆O_x species is provided in the supporting (Scheme S5).
495 As can be seen from there, an autoxidation mechanism can start from [•]C₁₀H₁₅O₄ and [•]C₁₀H₁₅O₆, yielding odd-oxygen
496 compounds shown in Table 4. For even-oxygen compounds, one could propose they are formed after production of
497 RO[•], through reaction R3 (Fig. S3) or decomposition of ROOH to yield RO[•] and OH[•], and also through oxidation of
498 [•]C₁₀H₁₇O₅ (Fig. S5). Products of additions of two oxygens ~~isare~~ also observed for other chemical formulas ~~of~~within
499 this common dataset. ~~Therefore, it questions the possibility that these two~~To further investigate the possible formation
500 of common products through atmospheric and combustion chemistries ~~develop autoxidation mechanisms with~~
501 ~~common isomers.~~

502 ~~In order to verify this possibility, considering the differences between limonene and α -pinene, we analyzed by~~
503 UHPLC-HRMS ~~experiments were performed.~~ The chemical compounds C₁₀H₁₆O₂ for limonene and C₁₀H₁₆O₃ for α -
504 pinene ~~in the samples from the combustion experiments. For limonene and α -pinene, were selected~~ considering the
505 availability of standards from suppliers, ~~we selected limonoaldehyde and pinonic acid, respectively. These two isomers~~
506 ~~of C₁₀H₁₆O₂ and C₁₀H₁₆O₃ are~~were among the most frequently reported products in atmospheric chemistry studies
507 (Table 45). Our study shows same retention times for these standards and isomers detected in combustion samples
508 (Fig S4S6). This result is more obvious for limonoaldehyde (11.5 min) than for pinonic acid (3.9 min). In addition, we
509 detected the presence of -OH or -OOH groups by H/D exchange with D₂O ~~for these two chemical formulas and C=O~~
510 ~~groups through derivatization of carbonyls with 2,4-DNPH for these two chemical formulas (Fig. S7). The low~~
511 ~~intensity of H/D exchange for α -pinene oxidation products indicates that the pinonic acid isomer is probably present~~
512 ~~at low concentration in the sample.~~ Unfortunately, coelution did not fully allow exploiting MS/MS fragmentation
513 carried out on the two chemical formulas, and to formally identify the two compounds. There is still a lot of
514 characterization work to be done, but the hypothesis of common isomeric products formed through an autoxidation
515 mechanism operating in atmospheric and low-temperature combustion conditions seems to be confirmed.

516 **Table 45.** Isomers of α -pinene and limonene oxidation reported in the literature.

	C ₁₀ H ₁₆ O ₂		C ₁₀ H ₁₆ O ₃	
α -pinene	Pinonaldehyde	(Fang et al., 2017)	Pinonic acid	(Fang et al., 2017;Ng et al., 2011;Meusinger et al., 2017)
	hydroxyketone	(Fang et al., 2017)	hydroxy pinonaldehydes	(Fang et al., 2017;Meusinger et al., 2017)
Limonene	limonoaldehyde	(Fang et al., 2017;Walser et al., 2008;Bateman et al., 2009)	limonic acid	(Fang et al., 2017;Witkowski and Gierczak, 2017;Hammes et al., 2019;Walser et al., 2008;Bateman et al., 2009;Warscheid and Hoffmann, 2001)
	4-isopropenyl-methylhydroxy-2-oxocyclohexane	(Fang et al., 2017)	7-hydroxy-limononaldehyde	(Fang et al., 2017;Walser et al., 2008;Bateman et al., 2009;Meusinger et al., 2017)

517

518 5 Conclusion

519 The oxidation of limonene-oxygen-nitrogen and α -pinene-oxygen-nitrogen mixtures was carried out using a jet-stirred
520 reactor at elevated temperature (590 K), a residence time of 2 s, and atmospheric pressure. The products were analyzed
521 by liquid chromatography, flow injection, and soft ionization-high resolution mass spectrometry. H/D exchange and
522 2,4-dinitrophenyl hydrazine derivatization were used to assess the presence of OOH and C=O groups in products,
523 respectively. We probed the effects of the type of ionization used in mass spectrometry analyses on the detection of
524 oxidation products. Heated electrospray ionization (HESI +/-) and atmospheric pressure chemical ionization (APCI
525 +/-) were used. A large dataset was obtained and compared with literature data obtained during the oxidation of
526 limonene and α -pinene under simulated tropospheric and low-temperature oxidation conditions. This work showed a
527 surprisingly similar set of chemical formulas of products, including oligomers, formed under the two rather different
528 conditions, i.e., cool flames and simulated atmospheric oxidation. Data analysis involving van Krevelen diagrams,
529 oxygen number distribution, oxidation state of carbon, and chemical relationship between molecules, indicated that a
530 subset of chemical formulas is common to all experiments independently of experimental conditions. More than 35%
531 of the chemical formulas detected in combustion chemistry experiments using a JSR have been detected in the studies
532 carried out under atmospheric conditions. Finally, we have outlined the existence of a substantial common dataset of
533 autoxidation products. This result tends to show that autoxidation is indeed inducing similarity between atmospheric
534 and combustion products. Detailed analysis of our data was performed by UHPLC-MS/MS of selected chemical
535 formulas observed in the literature. Nevertheless, final identification was not possible due to coelutions.

536 The present JSR data could be useful to atmospheric chemists working in the field of wildfire and/or biomass burning
537 induced air pollution. Considering that low-temperature oxidation (cool flame) products, i.e., VOCs, can be emitted
538 from biomass burning, wildfires and engine exhausts, the present data should be of interest for the atmospheric
539 chemists because they complement those obtained in atmospheric chemistry literature. It would be interesting to
540 complement the atmospheric relevant data with MS² analyses of products and assessment of the presence of
541 hydroperoxyl and carbonyl groups HOMs. Further MS² characterizations are also needed for the products observed in
542 the present work. Finally, a study of the temperature dependence of products formation would be very useful, both
543 under cool flame conditions and simulated atmospheric oxidation conditions.

544

545 Acknowledgements

546 The authors gratefully acknowledge funding from the Labex Caprysses (ANR-11-LABX-0006-01), the Labex
547 Voltaire (ANR-10-LABX-100-01), CPER, and EFRD (PROMESTOCK and APPROPOR-e projects) and the French
548 MESRI for a Ph.D. grant. We also thank (Tomaz et al., 2021) for sharing experimental data on limonene oxidation.

549

550 References

- 551 Bailey, H. C., and Norrish, R. G. W.: The oxidation of hexane in the cool-flame region, Proceedings of the Royal
552 Society of London Series a-Mathematical and Physical Sciences, 212, 311-330,
553 <https://doi.org/10.1098/rspa.1952.0084>, 1952.
- 554 Bateman, A. P., Nizkorodov, S. A., Laskin, J., and Laskin, A.: Time-resolved molecular characterization of
555 limonene/ozone aerosol using high-resolution electrospray ionization mass spectrometry, Physical Chemistry
556 Chemical Physics, 11, 7931-7942, <https://doi.org/10.1039/B905288G>, 2009.

- 557 Belhadj, N., Benoit, R., Dagaut, P., Lailliau, M., Serinyel, Z., Dayma, G., Khaled, F., Moreau, B., and Foucher, F.:
558 Oxidation of di-n-butyl ether: Experimental characterization of low-temperature products in JSR and RCM,
559 Combustion and Flame, 222, 133-144, <https://doi.org/10.1016/j.combustflame.2020.08.037>, 2020.
- 560 Belhadj, N., Benoit, R., Dagaut, P., and Lailliau, M.: Experimental characterization of n-heptane low-temperature
561 oxidation products including keto-hydroperoxides and highly oxygenated organic molecules (HOMs),
562 Combustion and Flame, 224, 83-93, <https://doi.org/10.1016/j.combustflame.2020.10.021>, 2021a.
- 563 Belhadj, N., Lailliau, M., Benoit, R., and Dagaut, P.: Towards a Comprehensive Characterization of the Low-
564 Temperature Autoxidation of Di-n-Butyl Ether, Molecules, 26, 7174, 2021b.
- 565 Belhadj, N., Lailliau, M., Benoit, R., and Dagaut, P.: Experimental and kinetic modeling study of n-hexane
566 oxidation. Detection of complex low-temperature products using high-resolution mass spectrometry, Combustion
567 and Flame, 233, 111581, <https://doi.org/10.1016/j.combustflame.2021.111581>, 2021c.
- 568 Benoit, R., Belhadj, N., Lailliau, M., and Dagaut, P.: On the similarities and differences between the products of
569 oxidation of hydrocarbons under simulated atmospheric conditions and cool flames, Atmos. Chem. Phys., 21,
570 7845-7862, <https://doi.org/10.5194/acp-21-7845-2021>, 2021.
- 571 Benson, S. W.: The kinetics and thermochemistry of chemical oxidation with application to combustion and flames,
572 Progress in Energy and Combustion Science, 7, 125-134, [https://doi.org/10.1016/0360-1285\(81\)90007-1](https://doi.org/10.1016/0360-1285(81)90007-1), 1981.
- 573 Bernath, P., Boone, C., and Crouse, J.: Wildfire smoke destroys stratospheric ozone, Science, 375, 1292-1295,
574 <https://doi.org/10.1126/science.abm5611>, 2022.
- 575 Berndt, T., Richters, S., Kaethner, R., Voigtländer, J., Stratmann, F., Sipilä, M., Kulmala, M., and Herrmann, H.:
576 Gas-Phase Ozonolysis of Cycloalkenes: Formation of Highly Oxidized RO₂ Radicals and Their Reactions with
577 NO, NO₂, SO₂, and Other RO₂ Radicals, The Journal of Physical Chemistry A, 119, 10336-10348,
578 <https://doi.org/10.1021/acs.jpca.5b07295>, 2015.
- 579 Berndt, T., Richters, S., Jokinen, T., Hyttinen, N., Kurtén, T., Otkjær, R. V., Kjaergaard, H. G., Stratmann, F.,
580 Herrmann, H., Sipilä, M., Kulmala, M., and Ehn, M.: Hydroxyl radical-induced formation of highly oxidized
581 organic compounds, Nat Commun, 7, 13677, <https://doi.org/10.1038/ncomms13677>, 2016.
- 582 Bianchi, F., Kurtén, T., Riva, M., Mohr, C., Rissanen, M. P., Roldin, P., Berndt, T., Crouse, J. D., Wennberg, P. O.,
583 Mentel, T. F., Wildt, J., Junninen, H., Jokinen, T., Kulmala, M., Worsnop, D. R., Thornton, J. A., Donahue, N.,
584 Kjaergaard, H. G., and Ehn, M.: Highly Oxygenated Organic Molecules (HOM) from Gas-Phase Autoxidation
585 Involving Peroxy Radicals: A Key Contributor to Atmospheric Aerosol, Chemical Reviews, 119, 3472-3509,
586 <https://doi.org/10.1021/acs.chemrev.8b00395>, 2019.
- 587 Burke, M., Driscoll, A., Heft-Neal, S., Xue, J., Burney, J., and Wara, M.: The changing risk and burden of wildfire
588 in the United States, Proceedings of the National Academy of Sciences, 118, e2011048118,
589 doi:10.1073/pnas.2011048118, 2021.
- 590 Camredon, M., Hamilton, J. F., Alam, M. S., Wyche, K. P., Carr, T., White, I. R., Monks, P. S., Rickard, A. R., and
591 Bloss, W. J.: Distribution of gaseous and particulate organic composition during dark α -pinene ozonolysis,
592 Atmos. Chem. Phys., <https://doi.org/10.5194/acp-10-2893-2010>, 2010.
- 593 Cox, R. A., and Cole, J. A.: Chemical aspects of the autoignition of hydrocarbon-air mixtures, Combust. Flame, 60,
594 109-123, [https://doi.org/10.1016/0010-2180\(85\)90001-X](https://doi.org/10.1016/0010-2180(85)90001-X), 1985.
- 595 Crouse, J. D., Nielsen, L. B., Jørgensen, S., Kjaergaard, H. G., and Wennberg, P. O.: Autoxidation of organic
596 compounds in the atmosphere, J. Phys. Chem. Lett., 4, 3513, 2013.
- 597 Dagaut, P., Cathonnet, M., Rouan, J. P., Foulatier, R., Quilgars, A., Boettner, J. C., Gaillard, F., and James, H.: A
598 jet-stirred reactor for kinetic studies of homogeneous gas-phase reactions at pressures up to ten atmospheres (\approx 1
599 MPa), Journal of Physics E: Scientific Instruments, 19, 207-209, <https://doi.org/10.1088/0022-3735/19/3/009>,
600 1986.
- 601 Dagaut, P., Cathonnet, M., Boettner, J. C., and Gaillard, F.: Kinetic Modeling of Propane Oxidation, Combustion
602 Science and Technology, 56, 23-63, <https://doi.org/10.1080/00102208708947080>, 1987.
- 603 Dagaut, P., Cathonnet, M., Boettner, J. C., and Gaillard, F.: Kinetic modeling of ethylene oxidation, Combustion and
604 Flame, 71, 295-312, [https://doi.org/10.1016/0010-2180\(88\)90065-X](https://doi.org/10.1016/0010-2180(88)90065-X), 1988.
- 605 Deng, Y., Inomata, S., Sato, K., Ramasamy, S., Morino, Y., Enami, S., and Tanimoto, H.: Temperature and acidity
606 dependence of secondary organic aerosol formation from α -pinene ozonolysis with a compact chamber system,
607 Atmos. Chem. Phys., 21, 5983-6003, <https://doi.org/10.5194/acp-21-5983-2021>, 2021.
- 608 Ehn, M., Thornton, J. A., Kleist, E., Sipilä, M., Junninen, H., Pullinen, I., Springer, M., Rubach, F., Tillmann, R.,
609 Lee, B., Lopez-Hilfiker, F., Andres, S., Acir, I. H., Rissanen, M., Jokinen, T., Schobesberger, S., Kangasluoma,
610 J., Kontkanen, J., Nieminen, T., Kurtén, T., Nielsen, L. B., Jørgensen, S., Kjaergaard, H. G., Canagaratna, M.,
611 Maso, M. D., Berndt, T., Petaja, T., Wahner, A., Kerminen, V. M., Kulmala, M., Worsnop, D. R., Wildt, J., and
612 Mentel, T. F.: A large source of low-volatility secondary organic aerosol, Nature, 506, 476-479,
613 <https://doi.org/10.1038/nature13032>, 2014.
- 614 Fang, W., Gong, L., and Sheng, L.: Online analysis of secondary organic aerosols from OH-initiated photooxidation
615 and ozonolysis of α -pinene, β -pinene, Δ 3-carene and d-limonene by thermal desorption-photoionisation aerosol
616 mass spectrometry, Environmental Chemistry, 14, 75-90, <https://doi.org/10.1071/EN16128>, 2017.

- 617 Gilman, J. B., Lerner, B. M., Kuster, W. C., Goldan, P. D., Warneke, C., Veres, P. R., Roberts, J. M., de Gouw, J.
618 A., Burling, I. R., and Yokelson, R. J.: Biomass burning emissions and potential air quality impacts of volatile
619 organic compounds and other trace gases from fuels common in the US, *Atmos. Chem. Phys.*, 15, 13915-13938,
620 <https://doi.org/10.5194/acp-15-13915-2015>, 2015.
- 621 Hammes, J., Lutz, A., Mentel, T., Faxon, C., and Hallquist, M.: Carboxylic acids from limonene oxidation by ozone
622 and hydroxyl radicals: insights into mechanisms derived using a FIGAERO-CIMS, *Atmos. Chem. Phys.*, 19,
623 13037-13052, <https://doi.org/10.5194/acp-19-13037-2019>, 2019.
- 624 Harvey, B. G., Wright, M. E., and Quintana, R. L.: High-Density Renewable Fuels Based on the Selective
625 Dimerization of Pinenes, *Energy Fuels*, 24, 267-273, <https://doi.org/10.1021/ef900799c>, 2010.
- 626 Harvey, B. G., Merriman, W. W., and Koontz, T. A.: High-Density Renewable Diesel and Jet Fuels Prepared from
627 Multicyclic Sesquiterpanes and a 1-Hexene-Derived Synthetic Paraffinic Kerosene, *Energy Fuels*, 29, 2431-
628 2436, <https://doi.org/10.1021/ef5027746>, 2015.
- 629 Hatch, L. E., Jen, C. N., Kreisberg, N. M., Selimovic, V., Yokelson, R. J., Stamatis, C., York, R. A., Foster, D.,
630 Stephens, S. L., Goldstein, A. H., and Barsanti, K. C.: Highly Speciated Measurements of Terpenoids Emitted
631 from Laboratory and Mixed-Conifer Forest Prescribed Fires, *Environmental Science & Technology*, 53, 9418-
632 9428, <https://doi.org/10.1021/acs.est.9b02612>, 2019.
- 633 Hecht, E. S., Scigelova, M., Eliuk, S., and Makarov, A.: Fundamentals and Advances of Orbitrap Mass
634 Spectrometry, *Encyclopedia of Analytical Chemistry*, 1-40, <https://doi.org/10.1002/9780470027318.a9309.pub2>,
635 2019.
- 636 Hu, Y., Fernandez-Anez, N., Smith, T. E. L., and Rein, G.: Review of emissions from smouldering peat fires and
637 their contribution to regional haze episodes, *International Journal of Wildland Fire*, 27, 293-312,
638 <https://doi.org/10.1071/WF17084>, 2018.
- 639 Huang, W., Saathoff, H., Pajunoja, A., Shen, X., Naumann, K. H., Wagner, R., Virtanen, A., Leisner, T., and Mohr,
640 C.: α -Pinene secondary organic aerosol at low temperature: chemical composition and implications for particle
641 viscosity, *Atmos. Chem. Phys.*, 18, 2883-2898, <https://doi.org/10.5194/acp-18-2883-2018>, 2018.
- 642 Iyer, S., Rissanen, M. P., Valiev, R., Barua, S., Krechmer, J. E., Thornton, J., Ehn, M., and Kurtén, T.: Molecular
643 mechanism for rapid autoxidation in α -pinene ozonolysis, *Nature Communications*, 12, 878,
644 <https://doi.org/10.1038/s41467-021-21172-w>, 2021.
- 645 Jokinen, T., Sipilä, M., Richters, S., Kerminen, V.-M., Paasonen, P., Stratmann, F., Worsnop, D., Kulmala, M., Ehn,
646 M., Herrmann, H., and Berndt, T.: Rapid Autoxidation Forms Highly Oxidized RO₂ Radicals in the Atmosphere,
647 *Angewandte Chemie International Edition*, 53, 14596-14600, <https://doi.org/10.1002/anie.201408566>, 2014a.
- 648 Jokinen, T., Sipilä, M., Richters, S., Kerminen, V. M., Paasonen, P., Stratmann, F., Worsnop, D., Kulmala, M., Ehn,
649 M., and Herrmann, H.: Rapid autoxidation forms highly oxidized RO₂ radicals in the atmosphere, *Angew.
650 Chem., Int. Ed.*, 53, 14596, 2014b.
- 651 Jokinen, T., Berndt, T., Makkonen, R., Kerminen, V.-M., Junninen, H., Paasonen, P., Stratmann, F., Herrmann, H.,
652 Guenther, A. B., Worsnop, D. R., Kulmala, M., Ehn, M., and Sipilä, M.: Production of extremely low volatile
653 organic compounds from biogenic emissions: Measured yields and atmospheric implications, *Proceedings of the
654 National Academy of Sciences*, 112, 7123-7128, <https://doi.org/10.1073/pnas.1423977112>, 2015.
- 655 Kekäläinen, T., Pakarinen, J. M. H., Wickström, K., Lobodin, V. V., McKenna, A. M., and Jänis, J.: Compositional
656 Analysis of Oil Residues by Ultrahigh-Resolution Fourier Transform Ion Cyclotron Resonance Mass
657 Spectrometry, *Energy Fuels*, 27, 2002-2009, <https://doi.org/10.1021/ef301762v>, 2013.
- 658 Khaykin, S., Legras, B., Bucci, S., Sellitto, P., Isaksen, L., Tencé, F., Bekki, S., Bourassa, A., Rieger, L., Zawada,
659 D., Jumelet, J., and Godin-Beekmann, S.: The 2019/20 Australian wildfires generated a persistent smoke-charged
660 vortex rising up to 35 km altitude, *Communications Earth & Environment*, 1, 22, [https://doi.org/10.1038/s43247-
661 020-00022-5](https://doi.org/10.1038/s43247-020-00022-5), 2020.
- 662 Kobziar, L. N., Pingree, M. R. A., Larson, H., Dreaden, T. J., Green, S., and Smith, J. A.: Pyroaerobiology: the
663 aerosolization and transport of viable microbial life by wildland fire, *Ecosphere*, 9, e02507,
664 <https://doi.org/10.1002/ecs2.2507>, 2018.
- 665 Korcek, S., Ingold, K. U., Chenier, J. H. B., and Howard, J. A.: Absolute rate constants for hydrocarbon autoxidation
666 .21. Activation-energies for propagation and correlation of propagation rate constants with carbon-hydrogen bond
667 strengths, *Canadian Journal of Chemistry*, 50, 2285-&, <https://doi.org/10.1139/v72-365>, 1972.
- 668 Kourtchev, I., Doussin, J. F., Giorio, C., Mahon, B., Wilson, E. M., Maurin, N., Pangui, E., Venables, D. S., Wenger,
669 J. C., and Kalberer, M.: Molecular Composition of Fresh and Aged Secondary Organic Aerosol from a Mixture
670 of Biogenic Volatile Compounds: A High-Resolution Mass Spectrometry Study, *Atmos. Chem. Phys.*, 15, 5683,
671 2015.
- 672 Krechmer, J. E., Groessl, M., Zhang, X., Junninen, H., Massoli, P., Lambe, A. T., Kimmel, J. R., Cubison, M. J.,
673 Graf, S., Lin, Y. H., Budisulistiorini, S. H., Zhang, H., Surratt, J. D., Knochenmuss, R., Jayne, J. T., Worsnop, D.
674 R., Jimenez, J. L., and Canagaratna, M. R.: Ion mobility spectrometry–mass spectrometry (IMS–MS) for on- and
675 offline analysis of atmospheric gas and aerosol species, *Atmos. Meas. Tech.*, 9, 3245-3262,
676 <https://doi.org/10.5194/amt-9-3245-2016>, 2016.

- 677 Kristensen, K., Watne, Å. K., Hammes, J., Lutz, A., Petäjä, T., Hallquist, M., Bilde, M., and Glasius, M.: High-
678 Molecular Weight Dimer Esters Are Major Products in Aerosols from α -Pinene Ozonolysis and the Boreal
679 Forest, *Environmental Science & Technology Letters*, 3, 280-285, <https://doi.org/10.1021/acs.estlett.6b00152>,
680 2016.
- 681 Kroll, J. H., Donahue, N. M., Jimenez, J. L., Kessler, S. H., Canagaratna, M. R., Wilson, K. R., Altieri, K. E.,
682 Mazzoleni, L. R., Wozniak, A. S., Bluhm, H., Mysak, E. R., Smith, J. D., Kolb, C. E., and Worsnop, D. R.:
683 Carbon oxidation state as a metric for describing the chemistry of atmospheric organic aerosol, *Nature*
684 *Chemistry*, 3, 133-139, <https://doi.org/10.1038/nchem.948>, 2011.
- 685 Kundu, S., Fisseha, R., Putman, A. L., Rahn, T. A., and Mazzoleni, L. R.: High molecular weight SOA formation
686 during limonene ozonolysis: insights from ultrahigh-resolution FT-ICR mass spectrometry characterization,
687 *Atmos. Chem. Phys.*, 12, 5523-5536, <https://doi.org/10.5194/acp-12-5523-2012>, 2012.
- 688 Kurtén, T., Rissanen, M. P., Mackeprang, K., Thornton, J. A., Hyttinen, N., Jørgensen, S., Ehn, M., and Kjaergaard,
689 H. G.: Computational Study of Hydrogen Shifts and Ring-Opening Mechanisms in α -Pinene Ozonolysis
690 Products, *The Journal of Physical Chemistry A*, 119, 11366-11375, <https://doi.org/10.1021/acs.jpca.5b08948>,
691 2015.
- 692 Melendez-Perez, J. J., Martínez-Mejía, M. J., and Eberlin, M. N.: A reformulated aromaticity index equation under
693 consideration for non-aromatic and non-condensed aromatic cyclic carbonyl compounds, *Organic Geochemistry*,
694 95, 29-33, <https://doi.org/10.1016/j.orggeochem.2016.02.002>, 2016.
- 695 Meusinger, C., Dusek, U., King, S. M., Holzinger, R., Rosenørn, T., Sperlich, P., Julien, M., Remaud, G. S., Bilde,
696 M., Röckmann, T., and Johnson, M. S.: Chemical and isotopic composition of secondary organic aerosol
697 generated by α -pinene ozonolysis, *Atmos. Chem. Phys.*, 17, 6373-6391, [https://doi.org/10.5194/acp-17-6373-](https://doi.org/10.5194/acp-17-6373-2017)
698 2017, 2017.
- 699 Mewalal, R., Rai, D. K., Kainer, D., Chen, F., Külheim, C., Peter, G. F., and Tuskan, G. A.: Plant-Derived Terpenes:
700 A Feedstock for Specialty Biofuels, *Trends Biotechnol.*, 35, 227-240,
701 <https://doi.org/10.1016/j.tibtech.2016.08.003>, 2017.
- 702 Ng, N. L., Canagaratna, M. R., Jimenez, J. L., Chhabra, P. S., Seinfeld, J. H., and Worsnop, D. R.: Changes in
703 organic aerosol composition with aging inferred from aerosol mass spectra, *Atmos. Chem. Phys.*, 11, 6465-6474,
704 <https://doi.org/10.5194/acp-11-6465-2011>, 2011.
- 705 Nørgaard, A. W., Vibenholt, A., Benassi, M., Clausen, P. A., and Wolkoff, P.: Study of Ozone-Initiated Limonene
706 Reaction Products by Low Temperature Plasma Ionization Mass Spectrometry, *Journal of The American Society*
707 *for Mass Spectrometry*, 24, <https://doi.org/1090-1096>, 10.1007/s13361-013-0648-3, 2013.
- 708 Nozière, B., Kalberer, M., Claeys, M., Allan, J., D'Anna, B., Decesari, S., Finessi, E., Glasius, M., Grgić, I.,
709 Hamilton, J. F., Hoffmann, T., Inuma, Y., Jaoui, M., Kahnt, A., Kampf, C. J., Kourtchev, I., Maenhaut, W.,
710 Marsden, N., Saarikoski, S., Schnelle-Kreis, J., Surratt, J. D., Szidat, S., Szmigielski, R., and Wisthaler, A.: The
711 Molecular Identification of Organic Compounds in the Atmosphere: State of the Art and Challenges, *Chemical*
712 *Reviews*, 115, 3919-3983, <https://doi.org/10.1021/cr5003485>, 2015.
- 713 Otkjær, R. V., Jakobsen, H. H., Tram, C. M., and Kjaergaard, H. G.: Calculated Hydrogen Shift Rate Constants in
714 Substituted Alkyl Peroxy Radicals, *The Journal of Physical Chemistry A*, 122, 8665-8673,
715 <https://doi.org/10.1021/acs.jpca.8b06223>, 2018.
- 716 Popovicheva, O. B., Engling, G., Ku, I. T., Timofeev, M. A., and Shonija, N. K.: Aerosol Emissions from Long-
717 lasting Smoldering of Boreal Peatlands: Chemical Composition, Markers, and Microstructure, *Aerosol and Air*
718 *Quality Research*, 19, 484-503, <https://doi.org/10.4209/aaqr.2018.08.0302>, 2019.
- 719 Prichard, S. J., O'Neill, S. M., Eagle, P., Andreu, A. G., Drye, B., Dubowy, J., Urbanski, S., and Strand, T. M.:
720 Wildland fire emission factors in North America: synthesis of existing data, measurement needs and management
721 applications, *International Journal of Wildland Fire*, 29, 132-147, <https://doi.org/10.1071/WF19066>, 2020.
- 722 Quéléver, L. L. J., Kristensen, K., Normann Jensen, L., Rosati, B., Teiwes, R., Daellenbach, K. R., Peräkylä, O.,
723 Roldin, P., Bossi, R., Pedersen, H. B., Glasius, M., Bilde, M., and Ehn, M.: Effect of temperature on the
724 formation of highly oxygenated organic molecules (HOMs) from alpha-pinene ozonolysis, *Atmos. Chem. Phys.*,
725 19, 7609-7625, <https://doi.org/10.5194/acp-19-7609-2019>, 2019.
- 726 Riva, M., Rantala, P., Krechmer, J. E., Peräkylä, O., Zhang, Y., Heikkinen, L., Garmash, O., Yan, C., Kulmala, M.,
727 Worsnop, D., and Ehn, M.: Evaluating the performance of five different chemical ionization techniques for
728 detecting gaseous oxygenated organic species, *Atmos. Meas. Tech.*, 12, 2403-2421, [https://doi.org/10.5194/amt-](https://doi.org/10.5194/amt-12-2403-2019)
729 [12-2403-2019](https://doi.org/10.5194/amt-12-2403-2019), 2019.
- 730 Savee, J. D., Papajak, E., Rotavera, B., Huang, H., Eskola, A. J., Welz, O., Sheps, L., Taatjes, C. A., Zádor, J., and
731 Osborn, D. L.: Carbon radicals. Direct observation and kinetics of a hydroperoxyalkyl radical (QOOH), *Science*,
732 347, 643-646, <https://doi.org/10.1126/science.aaa1495>, 2015.
- 733 Schneider, E., Czech, H., Popovicheva, O., Lütke, H., Schnelle-Kreis, J., Khodzher, T., Rüger, C. P., and
734 Zimmermann, R.: Molecular Characterization of Water-Soluble Aerosol Particle Extracts by Ultrahigh-
735 Resolution Mass Spectrometry: Observation of Industrial Emissions and an Atmospherically Aged Wildfire
736 Plume at Lake Baikal, *ACS Earth and Space Chemistry*, 6, 1095-1107,
737 <https://doi.org/10.1021/acsearthspacechem.2c00017>, 2022.

- 738 Seinfeld, J. H., and Pandis, S. N.: Atmospheric Chemistry and Physics: From Air Pollution to Climate Change, 2nd
739 ed., Wiley-Interscience, Hoboken, NJ, 1232 pp., 2006.
- 740 Smith, J. S., Laskin, A., and Laskin, J.: Molecular Characterization of Biomass Burning Aerosols Using High-
741 Resolution Mass Spectrometry, *Analytical Chemistry*, 81, 1512-1521, <https://doi.org/10.1021/ac8020664>, 2009.
- 742 Tomaz, S., Wang, D., Zabalegui, N., Li, D., Lamkaddam, H., Bachmeier, F., Vogel, A., Monge, M. E., Perrier, S.,
743 Baltensperger, U., George, C., Rissanen, M., Ehn, M., El Haddad, I., and Riva, M.: Structures and reactivity of
744 peroxy radicals and dimeric products revealed by online tandem mass spectrometry, *Nature Communications*, 12,
745 300, <https://doi.org/10.1038/s41467-020-20532-2>, 2021.
- 746 Tröstl, J., Chuang, W. K., Gordon, H., Heinritzi, M., Yan, C., Molteni, U., Ahlm, L., Frege, C., Bianchi, F., Wagner,
747 R., Simon, M., Lehtipalo, K., Williamson, C., Craven, J. S., Duplissy, J., Adamov, A., Almeida, J., Bernhammer,
748 A.-K., Breitenlechner, M., Brilke, S., Dias, A., Ehrhart, S., Flagan, R. C., Franchin, A., Fuchs, C., Guida, R.,
749 Gysel, M., Hansel, A., Hoyle, C. R., Jokinen, T., Junninen, H., Kangasluoma, J., Keskinen, H., Kim, J., Krapf,
750 M., Kürten, A., Laaksonen, A., Lawler, M., Leiminger, M., Mathot, S., Möhler, O., Nieminen, T., Onnela, A.,
751 Petäjä, T., Piel, F. M., Miettinen, P., Rissanen, M. P., Rondo, L., Sarnela, N., Schobesberger, S., Sengupta, K.,
752 Sipilä, M., Smith, J. N., Steiner, G., Tomè, A., Virtanen, A., Wagner, A. C., Weingartner, E., Wimmer, D.,
753 Winkler, P. M., Ye, P., Carslaw, K. S., Curtius, J., Dommen, J., Kirkby, J., Kulmala, M., Riipinen, I., Worsnop,
754 D. R., Donahue, N. M., and Baltensperger, U.: The role of low-volatility organic compounds in initial particle
755 growth in the atmosphere, *Nature*, 533, 527-531, <https://doi.org/10.1038/nature18271>, 2016.
- 756 Van Krevelen, D. W.: Graphical-statistical method for the study of structure and reaction processes of coal, *Fuel*, 29,
757 269-284, 1950.
- 758 Vereecken, L., Müller, J. F., and Peeters, J.: Low-volatility poly-oxygenates in the OH-initiated atmospheric
759 oxidation of α -pinene: impact of non-traditional peroxy radical chemistry, *Physical Chemistry Chemical
760 Physics*, 9, 5241-5248, <https://doi.org/10.1039/B708023A>, 2007.
- 761 Walser, M. L., Desyaterik, Y., Laskin, J., Laskin, A., and Nizkorodov, S. A.: High-resolution mass spectrometric
762 analysis of secondary organic aerosol produced by ozonation of limonene, *Physical Chemistry Chemical Physics*,
763 10, 1009-1022, <https://doi.org/10.1039/B712620D>, 2008.
- 764 Wang, Z., Popolan-Vaida, D. M., Chen, B., Moshhammer, K., Mohamed, S. Y., Wang, H., Sioud, S., Raji, M. A.,
765 Kohse-Höinghaus, K., Hansen, N., Dagaut, P., Leone, S. R., and Sarathy, S. M.: Unraveling the structure and
766 chemical mechanisms of highly oxygenated intermediates in oxidation of organic compounds, *Proceedings of the
767 National Academy of Sciences*, 114, 13102-13107, <https://doi.org/10.1073/pnas.1707564114>, 2017.
- 768 Wang, Z., Chen, B., Moshhammer, K., Popolan-Vaida, D. M., Sioud, S., Shankar, V. S. B., Vuilleumier, D., Tao, T.,
769 Ruwe, L., Bräuer, E., Hansen, N., Dagaut, P., Kohse-Höinghaus, K., Raji, M. A., and Sarathy, S. M.: n-Heptane
770 cool flame chemistry: Unraveling intermediate species measured in a stirred reactor and motored engine,
771 *Combustion and Flame*, 187, 199-216, <https://doi.org/10.1016/j.combustflame.2017.09.003>, 2018.
- 772 Wang, Z., Ehn, M., Rissanen, M. P., Garmash, O., Quéléver, L., Xing, L., Monge Palacios, M., Rantala, P.,
773 Donahue, N. M., Berndt, T., and Sarathy, M.: - Efficient alkane oxidation under combustion engine and
774 atmospheric conditions, *Communications Chemistry*, 4, 18, <https://doi.org/10.1038/s42004-020-00445-3>, 2021.
- 775 Warscheid, B., and Hoffmann, T.: Structural elucidation of monoterpene oxidation products by ion trap
776 fragmentation using on-line atmospheric pressure chemical ionisation mass spectrometry in the negative ion
777 mode, *Rapid Communications in Mass Spectrometry*, 15, 2259-2272, <https://doi.org/10.1002/rcm.504>, 2001.
- 778 Witkowski, B., and Gierczak, T.: Characterization of the limonene oxidation products with liquid chromatography
779 coupled to the tandem mass spectrometry, *Atmospheric Environment*, 154, 297-307,
780 <https://doi.org/10.1016/j.atmosenv.2017.02.005>, 2017.
- 781 Wotton, B. M., Gould, J. S., McCaw, W. L., Cheney, N. P., and Taylor, S. W.: Flame temperature and residence
782 time of fires in dry eucalypt forest, *International Journal of Wildland Fire*, 21, 270-281,
783 <https://doi.org/10.1071/WF10127>, 2012.
- 784 Xie, Q., Su, S., Chen, S., Xu, Y., Cao, D., Chen, J., Ren, L., Yue, S., Zhao, W., Sun, Y., Wang, Z., Tong, H., Su, H.,
785 Cheng, Y., Kawamura, K., Jiang, G., Liu, C. Q., and Fu, P.: Molecular characterization of firework-related urban
786 aerosols using Fourier transform ion cyclotron resonance mass spectrometry, *Atmos. Chem. Phys.*, 20, 6803-
787 6820, <https://doi.org/10.5194/acp-20-6803-2020>, 2020.
- 788 Zhang, H., Yee, L. D., Lee, B. H., Curtis, M. P., Worton, D. R., Isaacman-VanWertz, G., Offenberg, J. H.,
789 Lewandowski, M., Kleindienst, T. E., Beaver, M. R., Holder, A. L., Lonneman, W. A., Docherty, K. S., Jaoui,
790 M., Pye, H. O. T., Hu, W., Day, D. A., Campuzano-Jost, P., Jimenez, J. L., Guo, H., Weber, R. J., de Gouw, J.,
791 Koss, A. R., Edgerton, E. S., Brune, W., Mohr, C., Lopez-Hilfiker, F. D., Lutz, A., Kreisberg, N. M., Spielman,
792 S. R., Hering, S. V., Wilson, K. R., Thornton, J. A., and Goldstein, A. H.: Monoterpenes are the largest source of
793 summertime organic aerosol in the southeastern United States, *Proceedings of the National Academy of Sciences*,
794 115, 2038-2043, <https://doi.org/10.1073/pnas.1717513115>, 2018.
- 795 Zhao, Y., Thornton, J. A., and Pye, H. O. T.: Quantitative constraints on autoxidation and dimer formation from
796 direct probing of monoterpene-derived peroxy radical chemistry, *Proc Natl Acad Sci U S A*, 115, 12142-12147,
797 <https://doi.org/10.1073/pnas.1812147115>, 2018.